

Clusters in simple fluids

N. Sator¹

*Department of Physics and Astronomy, McMaster University, Hamilton, Ontario
L8S 4M1, Canada,*

*Dipartimento di Scienze Fisiche, INFN Napoli, Università di Napoli “Federico II”,
Complesso Universitario di Monte Sant’Angelo, Via Cintia, I-80126 Napoli, Italy*

Abstract

This article concerns the correspondence between thermodynamics and the morphology of simple fluids in terms of clusters. Definitions of clusters providing a geometric interpretation of the liquid-gas phase transition are reviewed with an eye to establishing their physical relevance. The author emphasizes their main features and basic hypotheses, and shows how these definitions lead to a recent approach based on self-bound clusters. Although theoretical, this tutorial review is also addressed to readers interested in experimental aspects of clustering in simple fluids.

Key words:

Clusters, Percolation, Liquid-gas phase transition

PACS: 64.60.Ak, 64.70.Fx, 36.40.Qv, 36.40.Ei, 61.20.Ne

Contents

1	Introduction	2
2	From thermodynamics to the morphology of simple fluids	3
3	Perfect gas of clusters	6
3.1	Mayer clusters	7
3.2	Frenkel clusters	8
3.3	Fisher droplets	9
4	Microscopic definitions of clusters in the lattice-gas model	14

Email address: sator@na.infn.it (N. Sator).

¹ Present address: Laboratoire de Physique Théorique des Liquides, Université Pierre et Marie Curie, 4, Place Jussieu 75252 Paris Cedex 05 France.

4.1	Ising clusters	16
4.2	Coniglio-Klein clusters	19
4.3	Swendsen-Wang clusters	23
5	Self-bound clusters	25
5.1	Definitions of self-bound clusters	26
5.2	Percolation lines in simple fluids	30
6	Summary and outlook	35
A	Perfect gas of clusters model	40
B	Stability of the probabilistic Hill clusters	43

1 Introduction

Simple fluids are classical systems in which chemically inert particles interact through a pairwise potential. The main features of the potential are the hard-core repulsion and the short-ranged attraction which give rise to thermal phase transitions. For example, noble gases and alkali metals are often modeled as simple fluids.

Moreover, attraction between particles promotes cluster formation. It is then sensible to look for a relation between thermodynamics and the morphology of a fluid in terms of clusters. In particular, a geometric interpretation of the liquid-gas phase transition is an important issue in statistical mechanics. To put it more precisely, there are two main issues: firstly to understand condensation as the sudden formation of a macroscopic cluster, and secondly to describe the morphology of the fluid at the critical point with a view to infer its thermodynamic properties.

To begin, it must be said that a geometric description of a fluid is outside the scope of thermodynamics. In addition to standard tools of thermal statistical physics, one has to define what is a cluster. At first sight, it may seem obvious to define a cluster as a set of particles close to each other and far from other clusters. However, this definition becomes quite ambiguous at high density, even below the critical density. Therefore, more sophisticated definitions of clusters were introduced, giving the geometric description of simple fluids a long and rich story.

This article presents a comprehensive review of proposed definitions of clusters,

with a view to establish a relation between thermodynamics and a geometric description of the fluid. However, the reader will see that this purpose will take us beyond this particular topic. On the one hand, our aim is to outline the main features of these various clusters. In particular, we highlight the hypotheses on which their definitions are built, in order to discuss their physical relevance. Indeed, some of these definitions were designed as mathematical tools to study thermodynamic properties. However, these clusters are often used in literature as though one could observe them experimentally. On the other hand, we clarify the relations between these definitions by following a chronological order so as to avoid frequent misunderstandings. Hence, we develop a new point of view about the Kertész line associated with the Coniglio-Klein clusters. From this standpoint, we present a recent approach in terms of self-bound clusters that provides a physical interpretation of the liquid-gas phase transition and suggests the existence of a percolation line in the supercritical phase of simple fluids.

This article is aimed not only at readers interested in fundamental aspects of the relation between thermodynamics and geometry, but also at experimentalists who deal with clusters in various fields of physics. In particular, we think of physicists who search for vestiges of phase transitions in small systems like atomic nuclei, and aggregates.

The plan of the review is as follows. In section 2, we recall the definition of a simple fluid and describe its typical phase diagram. Section 3 is devoted to definitions of clusters based on the “perfect gas of clusters model” developed in appendix A. Section 4 discusses microscopic definitions of clusters proposed in the framework of the lattice-gas model by means of percolation theory. In section 5, we are interested in self-bound clusters defined by energetic criteria. We present the correspondence between the phase diagram and their cluster size distribution, in the framework of the lattice-gas model, and by using numerical simulations of a Lennard-Jones fluid. Finally, section 6 contains a summary and we close by discussing several open questions.

2 From thermodynamics to the morphology of simple fluids

A simple fluid² is a classical system composed of N structureless particles of mass m , interacting through a two-body additive central potential $u(r_{ij})$, where r_{ij} is the distance between particles i and j . The potential must have a repulsive hard-core and a short range attraction that vanishes faster than $-1/r_{ij}^3$ to ensure the thermodynamic limit to exist in three dimensions (Ruelle,

² For a comprehensive review about simple liquids, we refer the reader to the book of Hansen and McDonald (1986).

1969). The Lennard-Jones potential, for instance, satisfies these conditions:

$$u(r_{ij}) = 4\epsilon\left[\left(\frac{\sigma}{r_{ij}}\right)^{12} - \left(\frac{\sigma}{r_{ij}}\right)^6\right] \quad (1)$$

where the two constants ϵ and σ fix the energy and length scales respectively. The Hamiltonian of the fluid is the sum of a kinetic and an interaction energy term:

$$\mathcal{H}(\{\vec{r}_i\}, \{\vec{p}_i\}) = \sum_{i=1}^N \frac{\vec{p}_i^2}{2m} + \sum_{i<j} u(r_{ij}) \quad (2)$$

where \vec{r}_i and \vec{p}_i are the position and momentum coordinates of the i^{th} particle, and $r_{ij} = |\vec{r}_i - \vec{r}_j|$. In the canonical ensemble, for a given volume V and temperature T , the partition function of the fluid is given by

$$Q_N(T, V) = \frac{1}{N!h^{3N}} \int e^{-\beta\mathcal{H}(\{\vec{r}_i\}, \{\vec{p}_i\})} d\vec{r}_1 \dots d\vec{r}_N d\vec{p}_1 \dots d\vec{p}_N$$

where $\beta = 1/kT$, k is the Boltzmann's constant and h the Planck's constant. Integrations over the momentum coordinates are straightforward and allow us to write the partition function as

$$Q_N(T, V) = \frac{1}{N!\lambda^{3N}} Z_N(T, V) \quad (3)$$

where

$$\lambda = \frac{h}{\sqrt{2\pi mkT}} \quad (4)$$

and

$$Z_N(T, V) = \int \prod_{i<j} e^{-\beta u(r_{ij})} d\vec{r}_1 \dots d\vec{r}_N. \quad (5)$$

Equation (4) defines the thermal wavelength. The thermodynamics of the fluid is then determined by the behaviour of the configuration integral $Z_N(T, V)$ in the thermodynamic limit.

The typical phase diagram of the system is shown in Fig. 1. In the $P - T$ diagram, coexistence curves separate the plane into three regions corresponding to the solid, liquid, and gas states. The liquid-gas coexistence curve stops at the critical point (C). Crossing this curve, the system undergoes a first order phase transition signaled by a latent heat and the coexistence of a low density

phase, the gas, and a high density phase, the liquid. In other words, compressing a gas at constant temperature T below the critical temperature T_c , a first drop of liquid appears when, in the phase diagram, one reaches the liquid-gas coexistence curve at the pressure $P_{cond}(T)$, at the corresponding density $\rho_{cond}(T)$. This phenomenon is called “condensation”. On the other hand, just at the critical point, a continuous phase transition occurs, while the compressibility and the specific heat diverge. The critical behaviour is known to be in the universality class of the Ising model (see for instance Goldenfeld, 1992). In the $T - \rho$ diagram, above the bell-shaped liquid-gas coexistence curve, there is one single fluid phase called the “supercritical phase”.³ Because the thermodynamic properties of the system vary smoothly along any path that does not cross a coexistence curve, it is possible to pass continuously from the gas to the liquid phase by following a path such as the dashed line shown in Fig. 1.

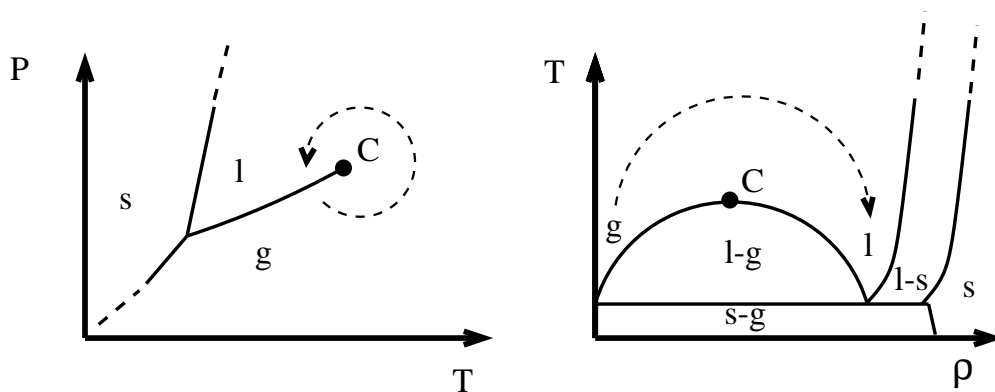


Fig. 1. Schematic phase diagram of a simple fluid in the $P - T$ plan (left) and the $T - \rho$ plan (right), where P , T and ρ are respectively the pressure, temperature and density of the system. The solid, liquid and gas phases are respectively noted s , l , and g . The critical point is C . The dashed line with the arrow represents a path in the phase diagram that does not lead to singularities of the partition function.

In the gas, liquid, and supercritical phases, the system is homogeneous, density is uniform on average. However, attractive interaction between particles contributes to forming localized morphological structures, the clusters. It must be emphasized that in order to study the morphology of a fluid, we need to give a definition of clusters in addition to standard thermodynamic tools. Indeed, the partition function depends only on the sum of the two-particle interactions, without discerning if a particle belongs to a cluster or not. In other words, one could arbitrary distribute the N particles among a set of clusters, while the partition function and all the thermodynamic properties would not be altered. Of course, the choice of the definition of clusters has no influence on the thermodynamic behaviour of the fluid, but depends on the problem we want to study.

³ The supercritical phase of a fluid (water) was discovered by the Baron Cagniard de La Tour (1822).

Historically, the first motivation for studying the morphology of a fluid was to interpret condensation as the sudden formation of a macroscopic cluster. At that time, the purpose was especially to determine thermodynamic quantities with the help of “effective” clusters used as a convenient and powerful tool. These first definitions of clusters are based on the “perfect gas of clusters model”.

3 Perfect gas of clusters

The basic idea is to assume that an imperfect fluid made up of interacting particles can be considered as a perfect gas of clusters at thermodynamic and chemical equilibrium: clusters do not interact with each other and do not have any volume. We shall discuss the validity of the perfect gas of clusters approximation at the microscopic level when we tackle the problem of self-bound clusters in section 5.2.

Let us suppose we deal with a collection of non-interacting clusters, without knowing how we can build them as sets of interacting particles. Clusters of given size s are characterized by their mass ms , a chemical potential μ_s , and a partition function $q_s(T, V)$. We show in appendix A that the pressure, the density, and the cluster size distribution, that is the mean number of clusters of size s , are respectively given by

$$\beta P = \frac{1}{V} \sum_{s=1}^{\infty} q_s z^s \quad (6)$$

$$\rho = \frac{1}{V} \sum_{s=1}^{\infty} s q_s z^s \quad (7)$$

$$n_s(T, z) = q_s z^s \quad (8)$$

where $z = e^{\beta\mu}$ is the fugacity and μ the particle chemical potential. The equation of state of the fluid can be obtained by eliminating z in the pressure expression with the help of Eq. (7). It is interesting to write Eq. (6) as a function of the cluster size distribution given by Eq. (8):

$$\beta PV = \sum_{s=1}^{\infty} n_s. \quad (9)$$

Equation (9) shows strikingly that the imperfect fluid can be seen as a perfect gas composed of $m_0 = \sum_{s=1}^{\infty} n_s$ non-interacting clusters.

According to Eqs. (6)-(8), thermodynamic quantities, as well as the cluster size distribution, are completely determined by the partition function of the

clusters. Now, two points of view can be considered. In the pioneer theory of condensation proposed by Mayer and his collaborators in 1937, clusters result from an exact enumeration of all the possible combinations of interacting particles (sec. 3.1). It is equivalent to giving a formal expression of $q_s(V, T)$ that is impracticable to handle for large size clusters. On the other hand, Frenkel, Band (sec. 3.2), and Fisher (sec. 3.3) propose a phenomenological expression of the partition function $q_s(V, T)$, and assume that clusters do not interact whatever the density.

3.1 Mayer clusters

Mayer’s theory of condensation is described in many textbooks of statistical physics (see for example Pathria, 1972; Huang, 1987) and in Mayer’s articles (Mayer, 1937; Mayer and Ackermann, 1937; Mayer and Harrison, 1938; Harrison and Mayer, 1938; Mayer and Mayer, 1940). Here, we just want to show how Mayer clusters can be seen as a particular case of the perfect gas of clusters model.

Originally, this theory was intended to express the exact equation of state of a real fluid, made up of interacting particles, as a series expansion in the density. To this end, Mayer decomposes the partition function (3) into the sum over all the possible partitions of particles into independent mathematical clusters. The first step is to introduce a function of the potential that is significant only if particles are close to each other:

$$f_{ij} = e^{-\beta u(r_{ij})} - 1.$$

The function $|f_{ij}|$ is bounded everywhere, unlike the potential $u(r_{ij})$, and tends to 0 when r_{ij} becomes large compared to the interaction range. Using this function as a small parameter, one can write the configuration integral (5) as a diagrammatic expansion by associating an N -particle graph with each term.⁴ A graph consists of vertices and bonds: to each particle corresponds a vertex, and the function f_{ij} is represented by a bond connecting vertices i and j . A set of pair by pair connecting vertices is called a “Mayer cluster”. Each graph, or term of the expansion, is characterized by a cluster size distribution.

By collecting the terms having the same cluster size distribution, one obtain a new expression of the partition function that can be simplified by moving over to the grand canonical ensemble. In the thermodynamic limit, pressure and density are eventually written as series expansion in the fugacity. As a result, calculations lead to the expressions (6) and (7), in which q_s/V is replaced by

⁴ According to Huang (1987), this is the first graphical representation of a perturbation series expansion in physics.

$\tilde{b}_s(T)/\lambda^3$, where coefficients $\tilde{b}_s(T)$ are the so-called “cluster integrals” introduced by Mayer, and λ is the thermal wavelength of the particle defined by Eq. (4).

In order to locate the condensation point, that is the density at which a macroscopic cluster appears, we have to examine the cluster size distribution given by Eq. (8). At a given temperature, the behaviour of the coefficients $\tilde{b}_s(T)$ for $s \gg 1$ shows that with increasing density, $n_s(T, \rho)$ becomes non-zero when $\rho > \rho_{cond}$. A macroscopic cluster appears, and Mayer identifies this particular density ρ_{cond} with the density of condensation. However, Yang and Lee (1952) proved that Mayer’s theory is exact in the gas phase, for $\rho < \rho_{cond}$, but cannot be carried forward into the liquid phase.

By definition, Mayer clusters form a perfect gas of clusters and are designed to evaluate thermodynamic quantities. Yet, it can be shown that $\tilde{b}_s(T)$, and therefore the cluster size distribution, may be negative in certain thermodynamic conditions. There then appears to be no physical interpretation of these clusters (Fisher, 1967a; Pathria, 1972).

3.2 Frenkel clusters

In contrast to Mayer’s theory, the basic idea of Frenkel’s model⁵ (Frenkel, 1939a,b) is to use directly the perfect gas of cluster model by choosing a phenomenological expression of the partition function of clusters. Afterward, this model was modified to allow for the volume of the clusters (Band, 1939b; Stillinger, 1963), but attraction between clusters was still overlooked.

By disregarding the degrees of freedom associated with the particles, Frenkel assumes the clusters of size s to be compact and writes their potential energy Ep_s , for s sufficiently large, as the sum of a bulk and a surface term

$$Ep_s(T) = -e_v s + e_a s^{\frac{2}{3}} \quad \text{for} \quad s \gg 1$$

where $e_v > 0$ and $e_a > 0$ are the bulk and surface potential energy by particle respectively. Frenkel does not take into account the entropy of the clusters and infers the partition function by integrating over the position and momentum coordinates of the center of mass of the cluster:

$$q_s(T, V) = V \left(\frac{\sqrt{s}}{\lambda} \right)^3 e^{-\beta Ep_s} = \frac{V}{\lambda^3} s^{\frac{3}{2}} e^{\beta(e_v s - e_a s^{\frac{2}{3}})}$$

⁵ A similar model has been independently proposed by Bijl (1938) and Band (1939a).

where λ/\sqrt{s} is the thermal wavelength of a cluster of size s (see Eq. (4)). According to Eq. (8), the Frenkel cluster size distribution is given by

$$\frac{n_s(T, z)}{V} = \frac{s^{\frac{3}{2}}}{\lambda^3} y^s x s^{\frac{2}{3}} \quad (10)$$

with

$$y(T, z) = z e^{\beta e_v} \quad \text{and} \quad x(T) = e^{-\beta e_a}.$$

The function y depends on the temperature and the density through z . The function x is independent of the density and always less than 1. For a given temperature T , x is fixed, the cluster size distribution depends on density only through $y(T, z)$. When $y < 1$, n_s decreases exponentially for $s \gg 1$: there is no macroscopic cluster, this corresponds to the gas phase. For $y > 1$, n_s decreases as long as s is smaller than a particular size, and then increases exponentially: a macroscopic cluster appears, which indicates the formation of the liquid phase. The density at the condensation point is then $\rho = \rho_{cond}(T)$ such that $y = y_{cond} = 1$.

The results of Frenkel's phenomenological model are for the most part the same as those of the Mayer's theory of condensation. The main advantage is that Frenkel clusters do not have the pathology of the Mayer clusters: the cluster size distribution (10) is positive whatever the temperature and density. However, this model does not allow one to locate the critical point and describe the morphology of the fluid in this state.

3.3 Fisher droplets

As Frenkel's model, Fisher's droplet model (Fisher, 1967a,b, 1971) is based on the perfect gas of clusters approximation. However, Fisher writes the partition function of the clusters of size s with the help of additional features: he allows for the entropy of the clusters, clusters are not assumed to be compact, and a corrective term varying like $\ln s$ is added to the free energy of the clusters of size s , in addition to the surface and volume terms.

Here, we shall not follow Fisher's original calculations (Fisher, 1967a). We rather propose a simplified and more direct way of calculating the partition function of clusters of size s (Fisher, 1971).

Let us first write the free energy of the clusters of size s . The mean internal energy and entropy of a cluster of size $s \gg 1$, with a mean surface area A_s , are written as the sum of a surface and volume term:

$$U_s = -u_v s + u_a A_s$$

$$S_s = s_v s + s_a A_s$$

where $u_v > 0$ and $s_v > 0$ are the volume energy and entropy by particle respectively, and $u_a > 0$ and $s_a > 0$, the surface energy and entropy by particle. Fisher does not assume the clusters to be compact and introduces a parameter σ to characterize the mean surface of the clusters of size s :

$$A_s(T) = a_0(T) s^\sigma \quad \text{with} \quad 0 < \sigma < 1.$$

The surface of a three-dimensional cluster should lie between the surface of a compact object ($\sigma = 2/3$) and the surface of a chain ($\sigma = 1$). Values of σ less than $2/3$ are interpreted by Fisher as an effective evaluation of the interaction between clusters.

Fisher also adds to the free energy a corrective logarithmic term which has no obvious physical interpretation⁶ (Binder, 1976b). The weight of this term is given by a second parameter τ . We shall see later that this term plays a crucial role in this model. The free energy $F_s(T, V)$ of a cluster of size s is then given by

$$-\beta F_s(T, V) = \beta(u_v + s_v T)s - \beta a_0(u_a - s_a T)s^\sigma - \tau \ln s + \ln c_0 V.$$

The term proportional to $\ln V$ results from the integration over the position of the center of mass of the cluster and c_0 is a constant. The partition function of a cluster of size s is eventually given by

$$q_s(T, V) = e^{-\beta F_s(T, V)} = c_0 V s^{-\tau} e^{\beta(u_v + s_v T)s - \beta a_0(u_a - s_a T)s^\sigma}.$$

On the basis of the “perfect gas of clusters model” presented in appendix A, the pressure, density, and the cluster size distribution are written as

$$\beta P \equiv \pi(T, z) = \frac{1}{V} \sum_{s=1}^{\infty} q_s z^s = c_0 \sum_{s=1}^{\infty} y^s x^{s^\sigma} s^{-\tau} \quad (11)$$

$$\rho = \frac{1}{V} \sum_{s=1}^{\infty} s q_s z^s = c_0 \sum_{s=1}^{\infty} s y^s x^{s^\sigma} s^{-\tau} \quad (12)$$

$$\frac{n_s}{V} = \frac{q_s}{V} z^s = c_0 y^s x^{s^\sigma} s^{-\tau} \quad (13)$$

where

$$y(T, z) = z e^{\beta(u_v + s_v T)}$$

$$x(T) = e^{-\beta a_0(u_a - s_a T)}.$$

⁶ This term is supposed to allow for the surface undulation of the clusters (Essam and Fisher, 1963; Fisher, 1971).

Following Fisher, we have introduced the series $\pi(T, z)$ in Eq. (11) and we define the derivative of order n by

$$\pi^{(n)}(T, z) = \left(z \frac{\partial}{\partial z}\right)^{(n)} \pi(T, z) = c_0 \sum_{s=1}^{\infty} y^s x^{s^\sigma} s^{n-\tau}.$$

The condensation point is determined by the appearance of a macroscopic cluster. According to the value of x , two cases are possible: if $x < 1$, as in Frenkel's model, the density of the condensation point ρ_{cond} is given by $y = y_{cond} = 1$, that is $z_{cond} = e^{-\beta(u_v + s_v T)}$. On the other hand, if $x \geq 1$, the cluster size distribution increases when $y > 1$ and the series (11) and (12), which give the pressure and density, diverge. Therefore, condensation only happens when $x < 1$, that is for $T < T_c = u_a/s_a$. This upper limit on the condensation temperature is interpreted as the critical temperature. Consequently, Fisher's model is not valid for $T > T_c$ or $\rho > \rho_{cond}$ ($x > 1$ or $y > 1$).

Despite the basic approximation of the perfect gas of clusters model, Fisher extends the validity of his model to the case of high densities and studies the vicinity of the critical point. At the critical point, $y = x = 1$, the critical density is given by

$$\rho_c = \pi^{(1)}(T_c, z_{cond}) = c_0 \sum_{s=1}^{\infty} s^{1-\tau}.$$

The convergence of this series implies $\tau > 2$. The behaviour of the thermodynamic quantities in the neighbourhood of the critical point is obtained by moving over to the continuous limit. The series $\pi^{(n)}(T, z)$ can be written for $z = z_{cond}$:

$$\pi^{(n)}(T, z_{cond}) = c_0 \sum_{s=1}^{\infty} s^{n-\tau} x^{s^\sigma} \sim c_0 \int_0^{\infty} s^{n-\tau} e^{-\theta s^\sigma} ds$$

where $\theta = \ln x^{-1} = \beta a_0 s_a (T_c - T)$. Performing the change of variable $t = \theta s^\sigma$, we have

$$\pi^{(n)}(T, z_{cond}) \sim \frac{c_0}{\sigma} \theta^{\frac{\tau-n-1}{\sigma}} \Gamma\left(\frac{n-\tau+1}{\sigma}\right) \sim (T_c - T)^{\frac{\tau-n-1}{\sigma}}.$$

We show in appendix A how thermodynamic quantities are linked to the derivatives $\pi^{(n)}$. According to the value of n , we infer the behaviour in the vicinity of the critical point of the specific heat C_v ($n = 0$), the density ($n = 1$), the compressibility χ ($n = 2$), and the pressure ($n = 0$):

$$\begin{aligned}
C_v &\sim (T_c - T)^{-\alpha_T} & \text{with} & \quad \alpha_T = 2 - \frac{\tau - 1}{\sigma} \\
\rho_c - \rho &\sim (T_c - T)^{\beta_T} & \text{with} & \quad \beta_T = \frac{\tau - 2}{\sigma} \\
\chi &\sim (T_c - T)^{-\gamma_T} & \text{with} & \quad \gamma_T = \frac{3 - \tau}{\sigma} \\
P_c - P &\sim (\rho_c - \rho)^{\delta_T} & \text{with} & \quad \delta_T = \frac{1}{\tau - 2}
\end{aligned} \tag{14}$$

Fisher's droplet model allows one to write the thermodynamic critical exponents α_T , β_T , γ_T , and δ_T as functions of the two geometric parameters σ and τ . Furthermore, the scaling relations between the thermal exponents (Fisher, 1967b), which had made this model well-known, follow easily from Eqs. (14):

$$\alpha_T + 2\beta_T + \gamma_T = 2 \tag{15}$$

$$\beta_T(\delta_T - 1) = \gamma_T. \tag{16}$$

Let us now show the relation between the thermodynamics and the geometric description of the fluid at the critical point. From Eq. (13), the cluster size distribution is written for $x = y = 1$

$$\frac{n_s}{V} = c_0 s^{-\tau}.$$

We now see that the term in $\ln s$, added by Fisher to the free energy, is essential at the critical point. Without this term, we cannot infer the scaling relations (15)-(16) and the power law behaviour of the cluster size distribution. It has to be pointed out that the relation between a power law cluster size distribution and the critical opalescence, observed at the critical point, is not clear today. A cautionary remark: this phenomenon, due to the divergence of the density fluctuations, is explained by thermodynamics without any reference to a geometric description of the fluid (Pathria, 1972; Chandler, 1987).

The two geometric exponents τ and σ can be written as functions of the thermodynamic critical exponents by reversing Eqs. (14):

$$\begin{aligned}
\sigma &= \frac{1}{\beta_T \delta_T} = \frac{1}{\beta_T + \gamma_T} \\
\tau &= 2 + \frac{1}{\delta_T} = 2 + \frac{\beta_T}{\beta_T + \gamma_T}.
\end{aligned}$$

In order to respect the critical behaviour of the thermodynamic quantities, exponents defined by Eqs. (14) must be positive. Consequently, the values of the geometric exponents are restricted to $2 < \tau < 3$, and $\sigma > 0.5$. Moreover,

the inflection point⁷ of the critical isotherm implies $\delta_T > 2$. Therefore, $2 < \tau < 2.5$, whatever the dimensionality (Kiang, 1970). The exponents τ and σ , calculated from the values of the thermodynamic exponents, are given in Table 1.

Table 1

Values of the thermodynamic critical exponents and of the Fisher exponents σ and τ at the critical point, in mean field theory and in the universality classes of the Ising model in 2 and 3 dimensions (from Goldenfeld, 1992).

	α_T	β_T	γ_T	δ_T	σ	τ
Mean field	0	1/2	1	3	2/3	7/3
2d-Ising	0	1/8	7/4	15	$8/15 \simeq 0.53$	$31/15 \simeq 2.07$
3d-Ising	0.12	0.325	1.24	4.8	0.64	2.21

The link between thermodynamics and a geometric description of the fluid stems from the perfect gas of clusters model. Indeed, Eqs. (A.6)-(A.8) of appendix A show that the first moments of the cluster size distribution are equal to thermodynamic quantities. For instance, moments of order 0, 1, and 2 behave respectively as the pressure, the density, and the compressibility. Therefore, the second moment of the droplet size distribution diverges like the compressibility at the critical point.

To test whether the droplet model is consistent with experimental data, the exponent τ can be indirectly evaluated by means of the compressibility factor $\beta P/\rho$, measured at the critical point (Kiang, 1970). Indeed, from Eqs. (11) and (12), we obtain for $x = y = 1$

$$\frac{P_c}{kT_c\rho_c} = \frac{\sum_{s=1}^{\infty} s^{-\tau}}{\sum_{s=1}^{\infty} s^{1-\tau}}. \quad (17)$$

For a large variety of real fluids, the value of τ inferred from Eq. (17) is in the order of 2.2, like the theoretical value calculated from the thermodynamic exponents (see Table 1). Moreover, a three-parameter fit of the compressibility factor along the coexistence curve provides a 1% agreement with experiment in the gas phase for water and carbon dioxide (Rathjen *et al.*, 1972).

However, we have to point out that Fisher’s model has some important weaknesses:

- Fisher droplets are “effective clusters” which form a perfect gas of clusters.⁸

⁷ In the vicinity of the critical point, $P_c - P \sim (\rho_c - \rho)^{\delta_T}$, and the second derivative of the pressure as a function of the density must vanish, then $\partial^2 P / \partial \rho^2 \sim (\rho_c - \rho)^{\delta_T - 2} = 0$. As a result, $\delta_T > 2$.

⁸ However, Stauffer and Kiang (1971) extended the droplet model by taking into

This basic assumption casts some doubt upon the adequacy of the model at high density. Besides, as far as we know, no attempt has been made to *observe* the Fisher droplets in a real system.

- The equation of state produces some singularities in the supercritical phase, which is forbidden by the theorems of Yang and Lee (1952) (Kiang and Stauffer, 1970).⁹
- The model does not describe the liquid phase beyond the coexistence curve for $\rho > \rho_{cond}$ (Kiang and Stauffer, 1970; Stauffer *et al.*, 1971).

Finally, despite these inadequacies, Fisher’s phenomenological model provides a first morphological interpretation of the critical point in terms of clusters, as well as a thermodynamic study of the condensation curve based on geometric arguments. During the past three decades, Fisher droplets have become a guide for defining physical clusters. Indeed, we have to *identify* clusters among the particles of the fluid, in order to compare theoretical results with experiments and numerical simulations. In brief, we need a microscopic definition of clusters that behave like Fisher droplets at the critical point.

4 Microscopic definitions of clusters in the lattice-gas model

The power law behaviour of the Fisher droplet size distribution and the divergence of the mean droplet size at the critical point remind those of a percolation phase transition.¹⁰ Reader not familiar with percolation theory is referred to the book by Stauffer and Aharony (1994). Hence, the works that followed those of Fisher have searched for a microscopic definition of clusters such that the thermodynamic critical point is a percolation threshold characterized by the Ising critical exponents. In other words, the microscopic clusters must verify the four following criteria at the critical point (Binder, 1976a; Kertész, 1989; Stauffer, 1990; Stauffer and Aharony, 1994):

- (1) The mean cluster size distribution behaves as a power law: $n_s \sim s^{-\tau}$ where τ is the Fisher exponent (see Table 1).
- (2) A percolating cluster appears and its size S_{max} varies like the order parameter of the thermal phase transition, i.e the density difference between liquid and gas (or the spontaneous magnetization in the Ising model), with the exponent β_T : $S_{max} \sim (T_c - T)^{\beta_T}$ for $T \leq T_c$.

account the excluded-volume and an additional attraction between the clusters as a small perturbation. Critical exponents are not affected by these corrections.

⁹ It is possible to cancel out these singularities by adding some corrective terms, without physical meaning, to the free energy of the clusters (Reatto, 1970).

¹⁰ Stillinger Jr (1963) put forward the idea for understanding the condensation as a percolation phase transition. In contrast, Fisher does not mention percolation in his original article (Fisher, 1967a).

- (3) The mean cluster size, i.e the second moment of the cluster size distribution¹¹ $S_{mean} \sim \sum_s s^2 n'_s$, diverges as the compressibility (or susceptibility) with the same exponent γ_T : $S_{mean} \sim |T - T_c|^{-\gamma_T}$.
- (4) The connectedness length diverges as the thermal correlation length with the same exponent ν_T .

We recall that in random percolation theory, the size of the largest cluster, the mean cluster size, the connectedness length, and the cluster size distribution are respectively described at the percolation threshold by the following critical exponents β_p , γ_p , ν_p , σ_p and τ_p . These exponents are universal for a given dimensionality and do not depend on the particular process of percolation (site/bond percolation, lattice/continuum space) (Stauffer and Aharony, 1994). For the sake of comparison, the thermodynamic and random percolation exponents are respectively given in Tables 1 and 2.

Table 2

Values of the critical exponents in mean field theory and in the universality classes of random percolation theory in 2 and 3 dimensions (from Stauffer and Aharony, 1994).

	β_p	γ_p	σ_p	τ_p
Mean field	1	1	1/2	5/2
2d-Percolation	0.139	2.39	0.39	2.05
3d-Percolation	0.41	1.80	0.45	2.18

The simplest and most natural way for defining and identifying clusters among a group of particles is to base the criterion on proximity in configurational space (Band, 1939a; Fisher, 1971): two particles are linked if the distance between them is shorter than a given cutoff distance b . A cluster is then a group of particles linked pair by pair¹² (see Fig. 2). In this article, such clusters will be denoted “configurational clusters”. We now have to choose the value of the cutoff distance. At very low density, the identification of clusters depends little on it. In contrast, this definition becomes very sensitive to the choice of b at higher densities (Stillinger, 1963; Lee *et al.*, 1973; Abraham and Barker, 1975; Binder, 1975). As an illustration, if we were to double the cutoff distance in Fig. 2, all the particles would belong to the same cluster.

¹¹ In percolation theory, the mean cluster size is usually defined as m_2/m_1 where $m_k = \sum_s s^k n'_s$ is the moment of order k of the cluster size distribution n'_s without the contribution of the largest cluster (Stauffer and Aharony, 1994).

¹² In the same spirit, a cluster can be defined either as particles lying inside a spherical shell centered on the center of mass of the cluster (Reiss *et al.*, 1968; Lee *et al.*, 1973; Abraham, 1974; Abraham and Barker, 1975), or as a density fluctuation exceeding a given threshold (Reiss *et al.*, 1990).

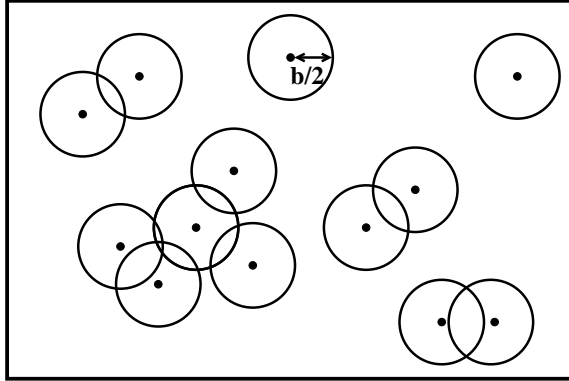


Fig. 2. *Particles in a box, in two dimensions. The radius of the discs centered at the positions of the particles is equal to $b/2$, where b is the cutoff distance. Configurational clusters are defined by the overlap of these discs. Hence, in this figure, one can see two monomers, three dimers and a cluster of size five.*

In order to apply the perfect gas of clusters model to a simple fluid, we could choose $b \simeq \text{constant} \times r_{min}$, where r_{min} is the distance corresponding to the minimum of the potential (Binder, 1975). Nevertheless, when a realistic potential is used, the attractive interaction between particles is never equal to zero, and there is no natural cutoff distance to defining the clusters: the choice of b is arbitrary.

Thanks to its simplicity, the lattice-gas (Ising) model is a suitable framework to study configurational clusters and to test the four criteria of the Fisher droplets at the critical point. As we shall see in the next section, by choosing an attraction only between particles occupying nearest neighbour sites of a lattice, it becomes natural to choose a cutoff distance equal to the finite range of the interaction (Stoll *et al.*, 1972; Binder, 1975; Müller-Krumbhaar and Stoll, 1976).

4.1 Ising clusters

First, let us recall the definition of the lattice-gas model. The M sites of a lattice are either empty or occupied by one of the N particles. Particles occupying nearest neighbour sites interact with an attractive energy $-\epsilon < 0$. The Hamiltonian is then given by

$$\mathcal{H} = \sum_{i=1}^M n_i \frac{p^2}{2m} - \epsilon \sum_{\langle i,j \rangle} n_i n_j$$

where $n_i = 0$ or 1, is the occupation number of the i^{th} site. Mass conservation implies

$$N = \sum_{i=1}^M n_i.$$

This Hamiltonian can be considered as a simplification of the simple fluid Hamiltonian given by Eq. (2). The equivalence of the lattice-gas model and the Ising model allows us to use the framework of the latter (Lee and Yang, 1952). An up spin is assigned to an occupied site, a down spin to an empty one, and a magnetic field H allows for the conservation (on average) of the number of particles. The interaction energy between two nearest neighbour up spins is $J = \epsilon/4$. The critical point is located at $T = T_c$, $\rho_c = 0.5$ in the lattice-gas model,¹³ and $H = 0$ in the Ising model. The line defined by $H = 0$ and $T < T_c$ in the phase diagram corresponds to the coexistence curve.

In the Ising model, configurational clusters are sets of nearest neighbour sites occupied by an up spin. For a given configuration of spins, the currently called “Ising clusters” are determined uniquely, as is shown in Fig. 3. By definition, Ising clusters are sets of interacting particles and there is no attraction between them. However, it must be emphasized that these clusters have an excluded volume which cannot be disregarded at high density. Consequently, unlike the Fisher droplets, Ising clusters do not make up a perfect gas of clusters.

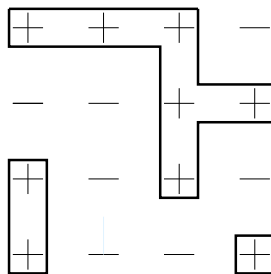


Fig. 3. Ising clusters on a square lattice. There is no (diagonal) bond between the next-nearest neighbour spins up.

The dimension d of configurational space has a crucial effect on thermal and geometric phase transitions. Therefore, the verification of the four Fisher criteria has to be considered according to the dimensionality.

In two dimensions: Coniglio and his collaborators (1977c) demonstrate by topological arguments that an infinite cluster appears exactly at the critical point. Numerical simulations on a square lattice exhibit a power law cluster size distribution characterized by an exponent $\tau = 2.1 \pm 0.1$ in agreement with Fisher’s model (Stoll *et al.*, 1972). On the other hand, a renormalization group

¹³ By spin up/spin down or particle/hole symmetry, the critical density of the lattice-gas model equals to 0.5 regardless of, either the structure of the lattice, or the dimension of the configurational space.

calculation of exponent ν shows that the average radius of the Ising clusters diverges like the correlation length, that is $\nu = \nu_T$ (Klein *et al.*, 1978). The first and fourth Fisher criteria are fulfilled by the Ising clusters.

In contrast, the exponents γ and β , which give respectively the critical behaviour of the mean cluster size and the mean size of the largest cluster, do not have the expected values of the thermodynamic exponents. Indeed, Sykes and Gaunt (1976) show that $\gamma = 1.91 \pm 0.01$ (while $\gamma_T = 1.75$) by means of series expansion calculations at low temperature on a triangular lattice. Numerical simulations confirm this disagreement: $\gamma = 1.901$ (Fortunato, 2002) and $\beta = 0.052 \pm 0.030$ (while $\beta_T = 0.125$) (Jan *et al.*, 1982). In other words, the second and third Fisher criteria are not verified. In two dimensions Ising clusters do not behave like Fisher droplets.

In three dimensions, none of the four Fisher criteria are met. Along the co-existence curve (for $H = 0$), a percolating cluster appears at a temperature lower than the critical one (at a density $\rho < \rho_c = 0.5$) (Coniglio, 1975): at $T \simeq 0.94T_c$ and $\rho \simeq 0.25$ in the cubic lattice from numerical simulations (Müller-Krumbhaar, 1974a,b), and at $\rho \simeq 0.1$ in the face-centered cubic lattice from an analytical calculation (Sykes and Gaunt, 1976).

Let us now consider the behaviour of the Ising clusters in the supercritical phase. By using numerical simulations on a square lattice, Odakaki and his coworkers (1975) show that a percolation line¹⁴ divides the supercritical region of the $T - \rho$ phase diagram into two areas: at low density there are only small size clusters, compared to the size of the system, and at high density a macroscopic percolating cluster connects two opposite sides of the lattice. This percolation line is plotted in Fig. 4 for two lattices. In two dimensions, and only in two dimensions, the percolation line starts at the critical point. In the limit $T \rightarrow \infty$, this line tends toward a density equal to the random site percolation threshold q_c . Indeed, at high temperature, interaction between spins becomes negligible compared to thermal agitation. As a result, up spins (particles) are randomly distributed with a probability equal to the density and we find the particular case of the random site percolation (Coniglio *et al.*, 1977c). As we can see in Fig. 4, the percolation behaviour is almost independent of temperature. However, the positive slope shows that a short range attraction favors the formation of clusters at low temperature, compared to the random site percolation at infinite temperature.

Critical exponents that characterize the moments of the cluster size distribution in the vicinity of the percolation line are equal to the random percolation exponents. A calculation using the renormalization group on a triangular lattice shows that the cluster radius diverges with the exponent ν_p along the

¹⁴In a previous work, Stillinger Jr (1963) had suggested the existence of a percolation line in the supercritical phase.

percolation line (Klein *et al.*, 1978). On the other hand, numerical simulations provide $\beta = 0.145 \pm 0.027$ (whereas $\beta_p = 0.139$) (Odagaki *et al.*, 1975).

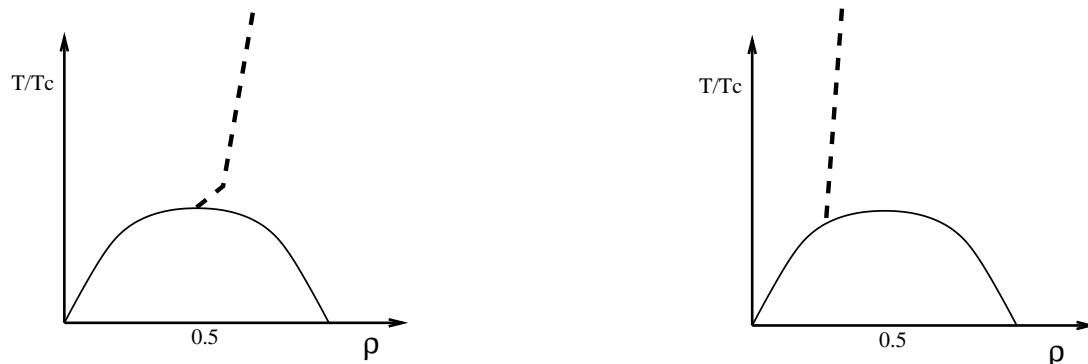


Fig. 4. Schematic phase diagram of the lattice-gas model. The coexistence curve (solid line) and the Ising clusters percolation line (dashed line) are represented for a square lattice ($q_c \simeq 0.59$) on the left, and for a cubic lattice ($q_c \simeq 0.31$), on the right. For a triangular lattice, $q_c = 0.5$: the percolation line is along the isochore $\rho = 0.5$ (see text for notation).

In an infinite Bethe lattice (mean field theory), Coniglio (1975; 1976) demonstrates that the percolation line does not start at the critical point, but at a lower density than the critical one, like in three-dimension lattices.

In conclusion, Ising clusters do not behave like Fisher droplets at the thermodynamic critical point, regardless of the dimensionality. Moreover, Ising clusters give rise to a percolation line in the supercritical phase. It is important to remark that the presence of a percolating Ising cluster in the supercritical phase was considered as non-physical, since on the basis of Fisher's model, it would imply thermodynamic singularities (Reatto, 1970; Binder, 1975; Müller-Krumbhaar and Stoll, 1976). We shall return to this point later, when we discuss Swendsen-Wang clusters (see section 4.3). Since Ising clusters are too large to behave like Fisher droplets, smaller clusters have to be defined (Binder, 1976a).

4.2 Coniglio-Klein clusters

Fortuin and Kasteleyn (Kasteleyn and Fortuin, 1969; Fortuin and Kasteleyn, 1972) propose a correspondence between thermodynamic and geometric quantities through a formalism based on graph theory within the framework of the Ising model. When the probability that two up spins are linked is properly chosen, the thermodynamic critical point is exactly a geometric critical point characterized by the exponents of the universality class of the Ising model.

Using an Hamiltonian formulation of random percolation based on an analytical extension of the Potts model (Wu, 1982) with x colors when $x \rightarrow 1$,

Coniglio and Klein (1980) obtain the same results as Fortuin and Kasteleyn, and define the so-called ‘‘Coniglio-Klein clusters’’. For a discussion about the relation between the approaches proposed by Fortuin and Kasteleyn and by Coniglio and Klein, we refer the reader to (Hu, 1984) and to the Appendix of (Coniglio, 2001). Two nearest neighbour sites occupied by an up spin are connected by a bond with the probability¹⁵

$$p_{ck}(\beta\epsilon) = 1 - e^{-\frac{\beta\epsilon}{2}}. \quad (18)$$

It is sometimes helpful to think of $1 - p_{ck}$ as the probability of breaking a bond between two nearest neighbouring up spins in an Ising cluster. Coniglio-Klein clusters are defined as sets of up spins linked by bonds.¹⁶ We remark that the probability p_{ck} is independent of the dimensionality. Figure 5 shows a configuration of Coniglio-Klein clusters obtained from the Ising clusters represented in Fig. 3. It must be emphasized that unlike Fisher droplets, Coniglio-Klein clusters do not form a perfect gas: besides having an hard-core repulsion like Ising clusters, they interact through nearest neighbouring up spins that are not connected by a bond, as illustrated in Fig. 5.

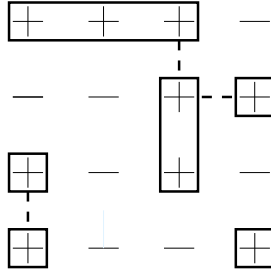


Fig. 5. A configuration of Coniglio-Klein clusters on a square lattice obtained from the Ising clusters of Fig. 3. The broken bonds between nearest neighbour up spins are represented by dashed lines.

In spite of this crucial difference, Coniglio-Klein clusters satisfy the four Fisher criteria at the critical point (Coniglio and Klein, 1980). Numerical simulations confirm this result and give for $H = 0$ and $T = T_c$, values of the geometric exponents equal to the thermodynamic ones: in two dimensions, an infinite cluster appears at the critical point (Ottavi, 1981), $\gamma = 1.77 \pm 0.03$ (while $\gamma_T = 1.75$), $\beta \simeq 0.125 = \beta_T$ (Jan *et al.*, 1982), and $\tau = 2.04$ (while the Fisher exponent is $\tau = 2.07$) (Liverpool and Glotzer, 1996). In three dimensions, Coniglio-Klein clusters diverge at the critical point (Stauffer, 1981) with $\gamma \simeq$

¹⁵ We choose to express p_{ck} in the lattice-gas framework. Because $J = \epsilon/4$, we have in the Ising model: $p_{ck} = 1 - e^{-2\beta J}$.

¹⁶ Following an idea of Binder (1976a), Alexandrowicz (1988; 1989) proposes to define clusters as sets of up (or down) spins surrounded by a perimeter of up and down spins at their average proportion. This leads to the same fractal dimension as the Coniglio-Klein’s definition at the critical point.

1.2 (while $\gamma_T = 1.24$), and $\tau \simeq 2.25$ (while the Fisher exponent is $\tau = 2.21$) (Roussenq *et al.*, 1982).

Coniglio-Klein clusters give rise to a new percolation line, known as the “Kertész line” or “Coniglio-Klein line”, which is shown in Fig. 6. As it should be, this line starts at the critical point ($\rho_c = 0.5$, $H = 0$) whatever the dimensionality, and reaches the point ($\rho = 1$, $H = \infty$) at temperature T_{bc} given by $1 - e^{-\frac{\epsilon}{2kT_{bc}}} = p_{bc}$, where p_{bc} is the random bond percolation threshold. Indeed, for $\rho = 1$, all the sites are occupied by an up spin (particle) and we find the particular case of random bond percolation (Heermann and Stauffer, 1981).

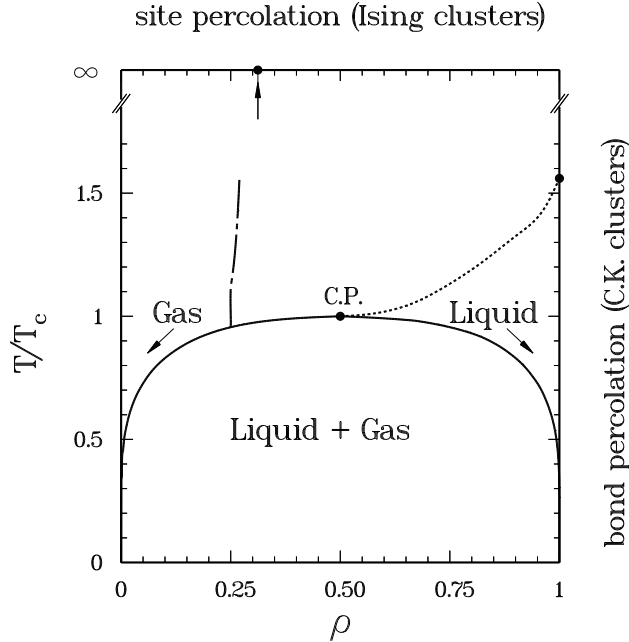


Fig. 6. Phase diagram $T - \rho$ of the lattice-gas model determined numerically in a simple cubic lattice. Coexistence curve (solid line). Critical point (C.P.). The Ising clusters percolation line (dashed-dotted line) ends at the site percolation threshold ($q_c \simeq 0.31$) when $T \rightarrow \infty$. The Coniglio-Klein percolation line, or Kertész line (dotted line), ends at the bond percolation threshold when $\rho = 1$ (from Campi and Krivine, 1997).

As we can see in Fig. 6, the supercritical area of the phase diagram is divided into a non-percolating region at high temperature and low density, and a percolating region at low temperature and high density. Along the Kertész line, geometric exponents are equal to those of random percolation (Coniglio and Klein, 1980; Stauffer, 1981). Therefore, values of geometric exponents pass discontinuously from the thermodynamic ones at the critical point, to

the random percolation values along the line, for $T > T_c$ and $\rho > \rho_c$ ($H > 0$).

It is interesting to remark that when interactions with next or second neighbours are taken into account, the critical point remains a geometric critical point for Coniglio-Klein clusters¹⁷ (Jan *et al.*, 1982). This result suggests that moving on to the continuum limit and considering a more realistic potential with a larger range of attraction, the critical point is a percolation threshold.¹⁸ This possibility, as well as the existence of a percolation line in a real fluid, will be discussed later on in section 5.

To close this subsection, we briefly discuss the behaviour of Coniglio-Klein and Ising clusters below the coexistence curve. At *thermal equilibrium*, Monte-Carlo simulations in three dimensions show that no critical percolation behaviour exists when phase separation occurs: critical percolation lines do not get into the two-phase region (Campi *et al.*, 2002a). Nevertheless, below the coexistence curve, there is always a macroscopic cluster (either a Coniglio-Klein or an Ising cluster), in the sense that a finite fraction of the particles belongs to the largest cluster.¹⁹ This is not the purpose of this review article to deal with the out of equilibrium and nucleation properties of simple fluids, however, we mention that Coniglio-Klein clusters, as well as Ising clusters, fulfill the phenomenological laws of Classical Nucleation Theory below the coexistence curve (Heermann *et al.*, 1984; Ray and Wang, 1990). On the other hand, in mean field theories, the compressibility diverges not only at the critical point but also along the well-defined spinodal line which separates the metastable and unstable regions. The mapping between thermodynamics and geometry in terms of Coniglio-Klein clusters cannot be extended into the metastable region (Schioppa *et al.*, 1998). However, by introducing the bond probability $P_B = 1 - e^{-\beta\epsilon(1-\rho)}$ between particles, the mean size of these new clusters diverges along the mean field spinodal line (Heermann *et al.*, 1984; Klein, 1990).

¹⁷ For Ising clusters, the density of the geometric critical point along the coexistence curve obviously decreases as the range of attraction increases (Bug *et al.*, 1985).

¹⁸ As a matter of fact, Fortuin and Kasteleyn's formalism has been generalized to the case of a short range potential in a continuous space (Drory, 1996).

¹⁹ To put it more precisely, the macroscopic cluster can be either too compact to span the system or enough spread out to percolate, according to temperature and density values. In the last case, although the largest cluster connects two opposite sides of the lattice, we recall that no critical percolation transition is observed, the distribution of finite size clusters remains exponentially decreasing and does not display any power law behaviour (Campi *et al.*, 2002a).

4.3 Swendsen-Wang clusters

As we have seen in the last section, Coniglio-Klein clusters behave like Fisher droplets at the critical point ($T = T_c$, $H = 0$). However, the percolation line in the supercritical phase ($T > T_c$, $H > 0$) was interpreted as a non-physical manifestation of these clusters. Within the context of the Fisher droplet model (or more generally in the perfect gas of clusters model), a percolation behaviour should imply singularities of thermodynamic quantities, which is forbidden in the supercritical phase by the theorems of Yang and Lee (1952). The aim was then to define clusters that have a geometric critical behaviour (percolation threshold) at, *and only at*, the thermodynamic critical point. In this spirit, the Kertész line was rather cumbersome (Coniglio *et al.*, 1989; Kertész, 1989; Stauffer, 1990).

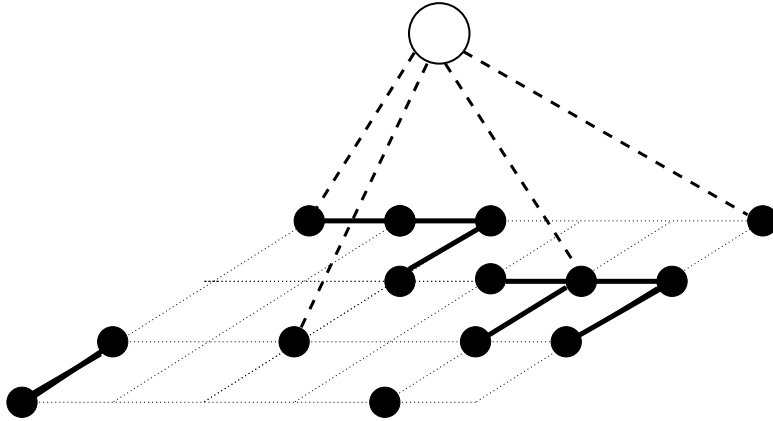


Fig. 7. Up Spins (particles) are represented in the lattice-gas formulation by a black dot. The white dot is the “ghost spin”. Bonds between up spins are active with probability $p_{ck} = 1 - e^{-2\beta J}$ (heavy line) and bonds between up spins and the “ghost spin” are active with probability $p_h = 1 - e^{-2\beta H}$ (dashed line). Some up spins are connected only through the “ghost spin”.

In order to get rid of the percolation line, Coniglio and his collaborators (1989), as well as Wang (1989), introduce a definition of clusters based on the work of Fortuin and Kasteleyn (Kasteleyn and Fortuin, 1969; Fortuin and Kasteleyn, 1972), and Swendsen and Wang²⁰ (1987). These so-called “Swendsen-Wang clusters” are defined like the Coniglio-Klein clusters, but in the presence of a positive (negative) magnetic field, H , up (down) spins are in addition connected to a “ghost spin” with the probability $p_h = 1 - e^{-|h|}$, where $h = 2\beta H$. This model is best explained by referring to Fig. 7. At each point of the phase diagram, the cluster *finite* size distributions of Swendsen-Wang clusters n_s^{sw} ,

²⁰ Swendsen-Wang algorithm, which allows one to reduce the critical slowing down at the critical point, is essentially based on the Fortuin and Kasteleyn’s formalism (Swendsen and Wang, 1987; Wang and Swendsen, 1990; Liverpool and Glotzer, 1996).

and Coniglio-Klein cluster n_s^{ck} , are related by (Wang, 1989):

$$n_s^{sw} = 2n_s^{ck} e^{-|h|s} \quad \text{where } s \text{ is finite.}$$

Hence, as soon as H is different from zero, a percolating cluster, which contains the ghost site, is present in the system whatever the temperature. Indeed, for $H > 0$, even if the magnetic field is weak, a macroscopic fraction ($1 - e^{-2\beta H} \simeq 2\beta H$) of up spins is connected to the “ghost spin”. As a result, there is a percolating cluster at each point of the phase diagram located above the coexistence curve (Stauffer, 1990; Adler and Stauffer, 1991). In the thermodynamic limit, any cluster that contains the “ghost spin” is infinite, and vice versa. The infinite cluster is unique. *Finite* Swendsen-Wang clusters behave as we expected: they verify the four Fisher criteria at the critical point, as the Coniglio-Klein clusters do. Besides, their mean size does not diverge in the supercritical phase. The percolation line is eliminated.

However, even if the finite Swendsen-Wang cluster size distribution does not have a power law behaviour in the supercritical phase, something happens along the Kertész line. Wang (1989) calculated n_s^{sw} , for large but finite clusters, by means of numerical simulations. According to the region of the phase diagram (see Fig. 6), he found:

- Above the Kertész line, $n_s^{sw} \sim e^{-c_1 s - |h|s}$
- Along the Kertész line, $n_s^{sw} \sim s^{-\tau} e^{-|h|s}$
- Below the Kertész line, $n_s^{sw} \sim e^{-c_2 s^{\frac{2}{3}} - |h|s}$

where the coefficients c_1 and c_2 depend on temperature and magnetic field. The Swendsen-Wang cluster size distribution decreases exponentially everywhere in the supercritical phase. However, the “surface term” of n_s^{sw} , varying like $s^{\frac{2}{3}}$ below the line, goes to zero along and above the line. Kertész (1989) and Stauffer (1990) suggested that the cancellation of the surface term in the expression for the cluster size distribution should imply a weak singularity of the cluster free energy.²¹ Discussing this result, Stauffer and Aharony (1994) wrote: “If correct, it would mean that we have to make more precise the century-old wisdom that nothing happens if we move continuously from the vapor to the liquid phase of a fluid by heating it above the critical temperature.”

At the beginning of the nineties, this claim sounded conclusive. Nevertheless, we believe this interpretation of the Kertész line to be incorrect and propose a new point of view. Indeed, it must be emphasized that this argument is based

²¹ According to Kertész (1989) the contribution of the percolating cluster to the total free energy should cancel out this weak singularity and the partition function would be of course analytical.

on the hypotheses of the perfect gas of clusters in which (see Eq. (8))

$$n_s = q_s z^s = e^{-\beta F_s + s \ln z} \quad (19)$$

Remember that Coniglio-Klein clusters, as well as Swendsen-Wang clusters, do not form a perfect gas of clusters. We can see therefore no valid reason for writing their cluster size distributions as Eq. (19). In other words, the particular behaviour of the Coniglio-Klein and Swendsen-Wang cluster size distributions along the Kertész line does not imply even weak thermodynamic singularities. Furthermore, as far as we know there is no physical interpretation of the ghost spin and Swendsen-Wang clusters. We shall see that this is not the case for Coniglio-Klein clusters.

Before we move on to the next section, we point out a general fact about clustering in simple fluids: the definition of clusters does depend on the physical problem we want to study. For example, Ising clusters do not provide a geometric interpretation of the liquid-gas transition. However, properties of electrical conductivity can be understood in terms of these clusters of interacting particles (Odagaki *et al.*, 1975; Yang and Thompson, 1998). Moreover, in the continuum case, configurational clusters have been used to describe the dynamics of hydrogen bonds in liquid water (Luzar and Chandler, 1996; Starr *et al.*, 1999).

5 Self-bound clusters

From now on, our purpose is to define clusters as self-bound sets of particles. A typical physical situation in which it is relevant to introduce “self-bound clusters” is the fragmentation of a piece of matter (such as an atomic nucleus, an atomic aggregate, or a liquid droplet) (Campi *et al.*, 2001a). In particular, a question of interest is the existence of *physical* clusters in a dense medium, before fragmentation occurs. This topic seems to contrast strongly with the discussion of the last sections. Yet, we shall see how such clusters can shed some light on the geometric interpretation of the liquid-gas phase transition.

Self-bound clusters would be stable if they were isolated from each other. In a dense medium, their definition cannot rest only on a criterion of proximity in configurational space. Such a definition would make no allowance for the relative motion of the particles. At high temperature, two particles that strongly interact are close to each other at a given time. Because of their high velocities, they may quickly move away from each other. A definition of clusters that takes into account the relative velocities of the particles corrects this

inadequacy.²²

In section 5.1, we present two definitions based on energetic criteria which allow us to identify self-bound clusters in a fluid knowing the positions and velocities of the particles. The first definition is global and based on minimizing the interaction energy between clusters. The second one is a local energetic criterion of bond activation. Next, we show that Coniglio-Klein clusters are self-bound on average. This crucial link between thermodynamics and the morphology of a fluid in the lattice-gas model will provide a geometric interpretation of the liquid-gas phase transition in terms of *physical* clusters. This point will be developed in section 5.2 for a Lennard-Jones fluid.

5.1 Definitions of self-bound clusters

5.1.1 A global criterion

At very low density, clusters are naturally defined as sets of particles that strongly interact with each other and do not interact (or only very loosely) with particles belonging to other clusters. This is the domain of validity of the perfect gas of clusters model.

In a dense fluid, by an argument of continuity, self-bound clusters can be defined by the partition of particles that minimizes the interaction energy (in absolute value) between clusters, or equivalently that minimizes the sum of the clusters internal energies. Indeed, the total energy E of the system divided in an arbitrary partition of clusters can be written

$$E = \sum_C \frac{1}{2} m N_C V_C^2 + \sum_C U_C + \sum_{C, C'} V_{int}(C, C') \quad (20)$$

where \sum_C is a sum over all the clusters, and N_C , U_C , and V_C are respectively the number of particles, the internal energy, and the velocity of the center of mass of cluster C . The term $V_{int}(C, C')$ is the interaction energy between clusters C and C' . We then have to find the partition of clusters that minimizes

$$U(P) = \sum_C U_C \quad (21)$$

This minimization problem has an exact, but not necessarily unique, solution.

²² An alternative approach is to introduce an arbitrary bond life time, in addition to the cutoff distance: two particles are linked if they remain within a certain distance during a given time (Pugnaloni *et al.*, 2000). However, not one but two adjustable parameters have to be chosen.

When the number of particles is small enough to enumerate all the possible partitions, a solution can be found easily. Otherwise, we can use two different methods for finding an optimal solution.

The first one was proposed by Dorso and Randrup (1993). It is based on an optimization procedure called “Simulated Annealing” (Kirkpatrick, 1984): consider an arbitrary partition of clusters P , a particle is randomly chosen and transferred from its original cluster C to another cluster C' . Of course, the particle remains at the same position in the fluid but we decide that it now belongs to another cluster. We obtain a new partition P' . The variation of the total internal energy between the two partitions is

$$\Delta U = U(P') - U(P) = U'_C + U'_{C'} - U_C - U_{C'}$$

where U'_C and $U'_{C'}$ are respectively the internal energies of clusters C and C' after the particle has been transferred. If $\Delta U < 0$, the partition P' is accepted. If $\Delta U > 0$, the partition P' is accepted with the probability $e^{-\frac{\Delta U}{T_e}}$, where T_e is a control parameter. The value of T_e is progressively decreased until there is no more modification of the cluster partition on a given number of attempts. As usual with Metropolis methods, the total internal energy of the final partition may be only a local minimum.

A second method, denoted “BFM“ (for Binary Fusion Method) has been developed by Puente (1999): initially, we suppose that there are only monomers in the fluid. The multiplicity, which is the number of clusters, is maximal, that is $m_0 = N$. Then, at each iteration we merge the two clusters that provide the lowest value of the function $U(P)$ (see Eq. (21)). The multiplicity is then reduced by one at each iteration. Therefore, at the first iteration a dimer is built, at the second either another dimer or a trimer, and so on. The process stops when the total internal energy cannot be reduced any more. This deterministic method follows a certain trajectory in the phase space of the partitions of clusters that does not necessarily lead to the optimal partition. On the other hand, the Simulated Annealing method can probe the phase space in a probabilistic way, which depends on arbitrary chosen parameters (like the number of Metropolis trials or the way T_e decreases). According to their authors, these two procedures provide clusters that are stable against particle emission. The definition of stability against particle emission is presented at the beginning of appendix B.

By means of numerical simulations of a Lennard-Jones fluid, Puente (1999) has shown that the Simulated Annealing and the BFM methods produce very similar cluster size distributions, but the last one is 10-20 times faster for the system considered. However, it has to be noted that both of these methods are very time consuming and cannot be used in practice for large systems made up of more than (say) $N = 1000$ particles.

5.1.2 A local criterion: Hill clusters

The definition of clusters proposed by Hill (1955) rests on a bond activation between pairs of particles. At a given time, two particles i and j , of respective velocities \vec{v}_i and \vec{v}_j , are linked if their relative kinetic energy K_r is lower than the negative of their attractive interaction energy $u(r_{ij})$:

$$K_r = \frac{m}{4}(\vec{v}_i - \vec{v}_j)^2 \leq -u(r_{ij}) \Rightarrow i \text{ and } j \text{ are linked.} \quad (22)$$

In other words, there is a bond between two particles if they are close enough to each other in the phase space, and not only in the configurational space. A Hill cluster is by definition a set of particles connected by bonds two by two. When the positions and velocities of the particles are known, for instance by means of molecular dynamics simulations (Allen and Tildesley, 1987), this local definition is completely deterministic and does not depend on adjustable parameters. It has to be noticed that the Hill's criterion can be used as well with Monte-Carlo calculations, although the velocities of the particles are not provided. Indeed, we checked by means of molecular dynamics simulations that mean cluster size distributions are not modified when we replace the velocity of each particle, provided by molecular dynamics simulations, with velocity components taken at random from a Gaussian distribution characterized by the temperature of the system (Sator, 2000). As far as mean cluster size distributions are concerned, position-velocity correlations are irrelevant and Monte-Carlo calculations can be used by allocating to each particle a velocity from a Gaussian distribution. Of course, time dependent properties and dynamics of the self-bound clusters are investigated only by molecular dynamics simulations.

A question that naturally arises at this point is the comparison between the global (Simulated Annealing and BFM) and the local (Hill) criterion. Performing molecular dynamics calculations with a Lennard-Jones fluid, Campi and his collaborators (Campi *et al.*, 2001a; Sator, 2000) have found that the cluster size distributions obtained with these three definitions are very similar. To quote Hill (1955): "A cluster is [...] a fairly definite physical concept so that all physically reasonable definitions should lead to rather similar predictions of the cluster size distribution." However, for a system of $N = 1000$ particles, Hill's criterion is 300 times faster to implement and can be used in practice for much larger systems, as we shall see in section 5.2.

Because it is arduous to carry out an analytical approach by using the Hill's criterion, it may be relevant to deal with a probabilistic formulation of the criterion (22). That requires us to calculate the probability that two particles are linked.

In a fluid at equilibrium, velocity components of the particles are given by a Gaussian distribution characterized by a variance $1/(\beta m)$, where m is the mass of the particles and $\beta = 1/kT$. The criterion (22) involves the relative kinetic energy between particles i and j which can be seen as the kinetic energy of a fictitious particle of reduced mass $\mu = m/2$ and relative velocity $\vec{v}_r = \vec{v}_i - \vec{v}_j$. The velocity components of the fictitious particle are then given by a Gaussian distribution with variance $2/\beta\mu = 1/\beta m$.

The probability $p_{Hill}(r, \beta)$ that two particles separated by a distance r are linked is then the probability that $K_r = \mu v_r^2/2 \leq -u(r)$, that is

$$\begin{aligned} p_{Hill}(r, \beta) &= \frac{\int_0^{\sqrt{-2u(r)/\mu}} v_r^2 e^{-\frac{\beta}{2}\mu v_r^2} dv_r}{\int_0^\infty v_r^2 e^{-\frac{\beta}{2}\mu v_r^2} dv_r} \\ &= \frac{\int_0^{\sqrt{-\beta u(r)}} x^2 e^{-x^2} dx}{\int_0^\infty x^2 e^{-x^2} dx} \\ &= \frac{\Gamma(\frac{3}{2}, -\beta u(r))}{\Gamma(\frac{3}{2})} \end{aligned}$$

where $\Gamma(n, x)$ is the incomplete gamma function. In this probabilistic framework, bonds are independent of each other, like in a random percolation process. As a consequence, we lose the velocity correlations between particles which are central in the deterministic criterion. We shall see in section 5.2 that clusters defined with the deterministic definition are much larger than the probabilistic clusters.

By using the probability $p_{Hill}(r, \beta)$, Hill (1955) introduced two effective potentials between bound and unbound pairs of particles for expressing the mean number of clusters as density and activity series expansions.²³ A very similar approach has been used recently to calculate the first order corrections (namely by considering the interaction between a monomer and a self-bound cluster) to the perfect gas of clusters at low density (Soto and Cordero, 1997). Coniglio and his collaborators (1977a; 1977b) extended the Hill's method and developed an integral equation theory of the pair connectedness function, which is proportional to the probability that two particles belong to the same cluster.²⁴ With an Ornstein-Zernike-type equation and a closure relation, like the Percus-Yevick approximation, the mean cluster size can be obtained from the integration of the pair connectedness function. Very recently, a generalization to the case of the deterministic Hill's criterion has been proposed and should provide interesting results (Pugnaloni *et al.*, 2000, 2002).

²³ This method, which takes into account the interactions between clusters, can be formally applied to any microscopic definition of clusters.

²⁴ For a comprehensive review about integral equation theory, see (Caccamo, 1996).

5.1.3 Coniglio-Klein and self-bound clusters

In the lattice-gas model, interaction is equal to $-\epsilon$ between nearest neighbour particles, and 0 otherwise. The probability that two nearest neighbour particles are linked becomes (Campi and Krivine, 1997)

$$\begin{aligned} p_{Hill}(\beta\epsilon) &= \frac{4}{\sqrt{\pi}} \int_0^{\sqrt{\beta\epsilon}} e^{-x^2} x^2 dx \\ &= 1 - \frac{4}{\sqrt{\pi}} \int_{\sqrt{\beta\epsilon}}^{\infty} x^2 e^{-x^2} dx. \end{aligned} \quad (23)$$

We show in appendix B that probabilistic Hill clusters are stable on average against particle emission. By performing a Laguerre expansion of Eq. (23), Campi and Krivine (1997) have found

$$\begin{aligned} p_{Hill}(\beta\epsilon) &= 1 - 0.911e^{-\frac{\beta\epsilon}{2}} - 0.177(1 - \beta\epsilon)e^{-\frac{\beta\epsilon}{2}} + \dots \\ &= p_{ck}(\beta\epsilon) - 0.088(1 - 2.01\beta\epsilon)e^{-\frac{\beta\epsilon}{2}} + \dots \\ &\simeq p_{ck}(\beta\epsilon) \end{aligned} \quad (24)$$

where $p_{ck}(\beta\epsilon) = 1 - e^{-\frac{\beta\epsilon}{2}}$ is the probability introduced by Coniglio and Klein (see section 4.2). Equation (24) shows that probabilities p_{ck} and p_{Hill} are very close to each other (for example at the critical point of the cubic lattice, the relative error between the two probabilities is less than 6%).²⁵ This is a crucial result: Coniglio-Klein clusters, which have been introduced specifically to provide a correspondence between geometric and thermodynamic critical behaviour, do have a physical interpretation in terms of self-bound clusters. Conversely, self-bound clusters give rise to a percolation line which starts at the critical point in the framework of the lattice-gas model.

5.2 Percolation lines in simple fluids

Numerical simulations of a Lennard-Jones fluid provide a more realistic theoretical framework than the lattice-gas model. With the help of canonical Monte Carlo and microcanonical molecular dynamics calculations (Allen and Tildesley, 1987), Campi and his collaborators (Sator, 2000; Campi *et al.*, 2001a) have studied systems made up of a large number of particles ($N = 11664$)

²⁵ Pan and Das Gupta (1995) had already noticed this similarity using numerical simulations.

interacting through a Lennard-Jones potential given by Eq. (1). The phase diagram of this simple fluid is presented in Fig. 8. It must be emphasized that the phase diagram, as well as the results we present below, are qualitatively insensitive to this particular choice of potential and can be considered as generic for simple fluids. To reduce the computer time calculation, self-bound clusters are recognized by using the local deterministic criterion proposed by Hill (see section 5.1.2).

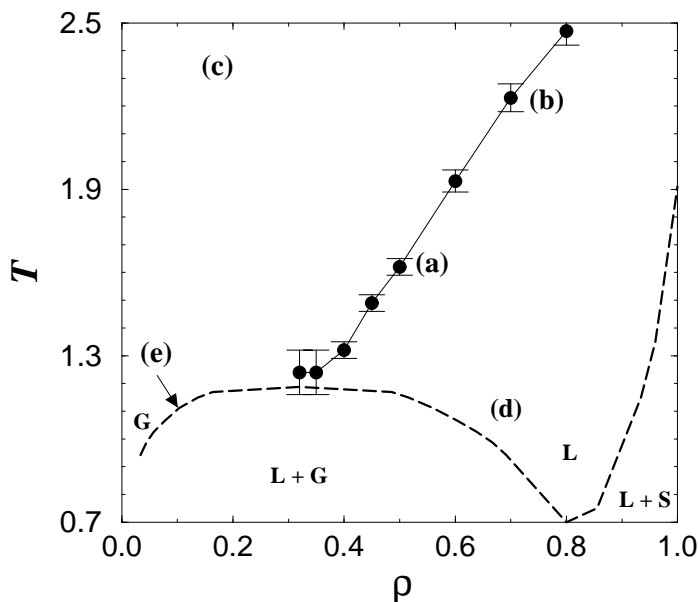


Fig. 8. Phase diagram of the Lennard-Jones fluid. The dashed line indicates the coexistence curves between the gas (G), liquid (L) and solid phases (S). The continuous line is the critical percolation line of self-bound clusters. Temperature T and density ρ are in units of ϵ and σ^{-3} respectively (see Eq. (1)) (from Campi et al., 2001a).

As a first result, a “macroscopic” cluster appears as soon as the liquid-gas phase transition takes place. Figure 9 represents two cluster size distributions plotted around the point (e) of the phase diagram (see Fig. 8), just above and just below the coexistence curve. We can see a drastic change in the mean number of large clusters which corresponds very well to the crossing of the coexistence curve. Obtained without any free parameter, this clean correspondence between thermodynamic and morphological changes cannot but support the physical nature of these clusters. It is important to note that along the coexistence curve, the cluster size distribution is not a power law and therefore, does not present a geometric (percolation) critical behaviour.

What is more, self-bound clusters give birth to a critical percolation line²⁶

²⁶ This line should not be confused with the Fisher-Widom line (Fisher and Widom, 1969), which divides the supercritical region into a gas-like and a liquid-like domain (with probably no relevance to clustering) according to the behaviour of the radial

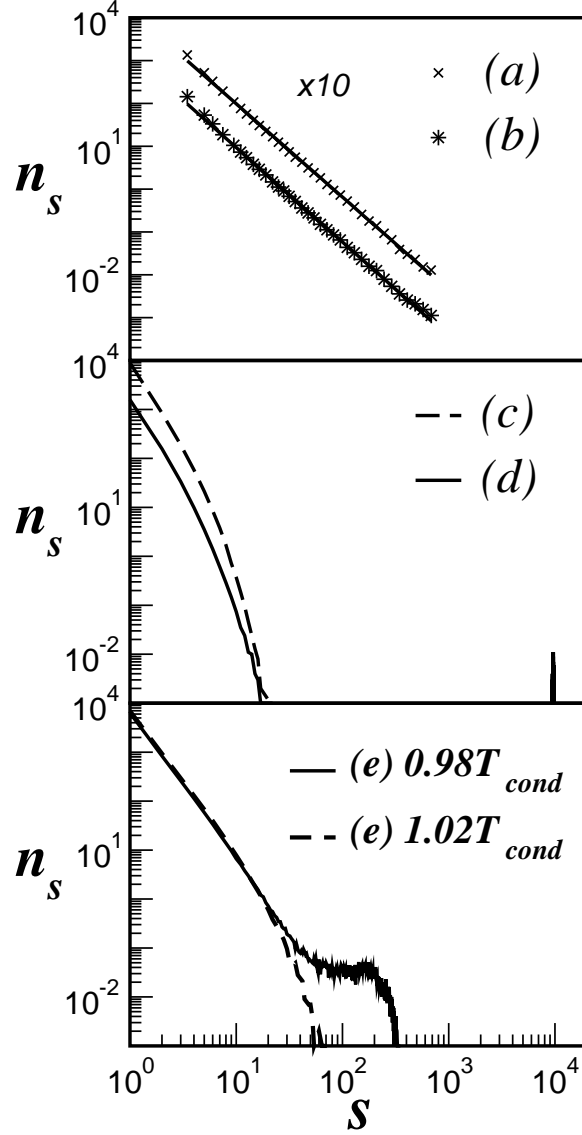


Fig. 9. Cluster size distributions n_s at points (a)-(b), (c)-(d) and (e) of the phase diagram (see Fig. 8). For curve (d): the contribution of the percolating cluster is sharply peaked around $s \simeq 9500$. For curves (e): T_{cond} is the temperature of condensation at $\rho = 0.1$ (from Campi et al., 2001a).

represented in Fig. 8. To illustrate this percolation behaviour, the cluster size distribution is plotted in Fig. 9 for several points of the phase diagram. Along the line the cluster size distribution behaves as a power law characterized by an exponent $\tau = 2.20 \pm 0.05$ (while in random percolation theory $\tau_p = 2.18$). The fractal dimension of the clusters, as well as the other exponents that characterize the moments of the cluster size distribution in the vicinity of

distribution function, nor with the extrapolation of the rectilinear diameter line (Nishikawa and Morita, 2000), which is the locus of points of maximum compressibility.

the line, are also in good agreement with those of random percolation theory (Campi *et al.*, 2001a; Sator, 2000). Yet, this result was found on a deterministic dynamical framework, without any explicit reference to a random (site or bond) percolation mechanism. This is even more striking when the global definition is used instead of the bond activation criterion.

The percolation line starts at the critical point, within error bars due to the finite size of the system and to critical slowing down. Just at this point, for the same technical reasons, geometric critical exponents were not evaluated with enough accuracy to distinguish between the universality classes of the Ising model and of the random percolation. Furthermore, the total energy of the system remains almost constant along the percolation line²⁷ (Campi *et al.*, 2001a). The origin of this energy invariance, which results from a subtle balance between internal, center of mass kinetic, and inter-cluster potential energies (see Eq. (20)), is not understood (Campi *et al.*, 2001b).

It is interesting to notice that along the condensation curve, and in particular at the critical point, self-bound clusters seem to behave like Fisher droplets. Hence, their cluster size distributions can be fitted by Eq. (13), which was proposed by Fisher. However, self-bound clusters do not form a perfect gas as Fisher droplets do, and there is absolutely no reason for writing their free energy as $-\beta F_s = \ln n_s - s \ln z$. Indeed, the contribution of the interaction between self-bound clusters to the total potential energy of the system is at least 40% along both the percolation line and the condensation curve (Sator, 2000). Even at very low density, such as $\rho \simeq 0.05$ in two dimensions, the interaction between a single monomer and a self-bound cluster markedly modifies the cluster size distribution of the ideal gas of clusters (Soto and Cordero, 1997). In addition, we recall that the definition of the self-bound clusters tends to minimize interaction between clusters. These results show strikingly that whatever microscopic definition of clusters is chosen, it is not realistic to treat them as a perfect gas of clusters, even at low densities $\sim \rho = \rho_c/3 \simeq 0.1$.

For a given cluster size s , the degrees of freedom associated with the motion of the particles inside the clusters, and the center of mass motion of the clusters, are respectively characterized²⁸ by an “internal effective temperature” $T^*(s)$ and a “translational effective temperature” $T^{cm}(s)$. Analytical calculations (Soto and Cordero, 1998a,b) as well as numerical simulations (Campi *et al.*, 2001b, 2002b) show that whatever the size of the clusters and the thermodynamical state of the system, $T^*(s) < T < T^{cm}(s)$ where T is the real thermodynamic temperature of the system. Simply put, the system can be seen as a

²⁷ The same observation has been made about the Kertész line in the lattice-gas model (Campi *et al.*, 1999).

²⁸ These effective temperatures, $T^*(s)$ and $T^{cm}(s)$, are defined as twice the corresponding average kinetic energy divided by the number of degrees of freedom, that is $3(s-1)$ and 3 respectively in three dimensions.

“hot” gas of “cold” physical clusters. This result, due to the self-bound nature of the clusters, is particularly relevant when studying the fragmentation and expansion of a small system. Indeed, once the clusters are isolated from each others, the internal effective temperature becomes the real temperature of a fragment in the microcanonical ensemble (Campi *et al.*, 2002b).

As we have seen in section 5.1.2, self-bound clusters can also be defined by a simplified probabilistic criterion. By means of molecular dynamics simulations of a Lennard-Jones fluid, Pugnaroni and his collaborators (2002) have recently shown that this definition strongly overestimates the percolation density by a factor 1.5-2, especially at high temperatures. In other words, probabilistic clusters are much smaller on average than the deterministic Hill clusters. On the other hand, the mean cluster size of the probabilistic Hill clusters can be calculated using an integral equation theory²⁹ (Coniglio *et al.*, 1977a). The percolation density is then determined by the divergence of the mean cluster size. When compared to the molecular dynamics results, the percolation line of the probabilistic clusters is shifted to much lower densities and may seem to roughly coincide with the percolation line of the deterministic clusters (Coniglio *et al.*, 1977a; Pugnaroni *et al.*, 2002).

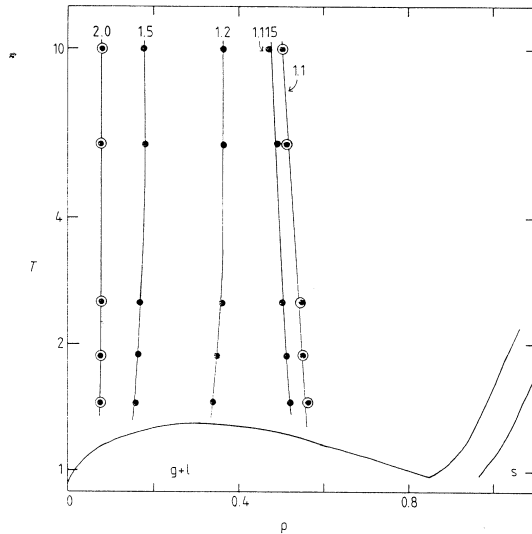


Fig. 10. Percolation lines of the configurational clusters in the $T-\rho$ phase diagram of a Lennard-Jones fluid determined by molecular dynamics simulations for two system sizes: $N = 108$ (black points) and $N = 500$ (circled points). The corresponding value of the cutoff distance b is indicated for each percolation line. Note that $b_{min} \simeq 1.12$ is the distance corresponding to the minimum of the Lennard-Jones potential (from Heyes and Melrose, 1988).

For completeness, we mention that configurational clusters (see section 4),

²⁹ Xu and Stell (1988) used this approach to study the percolation behaviour of a Yukawa fluid. However, clusters are defined either by a cutoff distance or by a probability of connection which depends on an adjustable parameter.

defined by a cutoff distance b , also generate a percolation line which almost follows an isochore ($\rho = cte$), as do Ising clusters in the lattice-gas model (Geiger and Stanley, 1982; Bug *et al.*, 1985; Safran *et al.*, 1985; Xu and Stell, 1988). Of course, the position of the line in the phase diagram depends crucially on the choice of b (Heyes and Melrose, 1988, 1989; Xu and Stell, 1988), as can be seen in figure 10.

In the very particular case of Baxter’s sticky-hard-sphere model (or adhesive-hard-sphere model) (Baxter, 1968), configurational clusters become identical to self-bound clusters. The potential is a hard spheres plus a square-well potential, in the limit where the depth of the well goes to infinity, and its width goes to zero, in such a way that the product of depth and width remains constant. The cutoff distance b is then obviously the diameter of the core. Besides, once in contact, two particles are permanently bound. Baxter (1968) solved this model analytically, using the Ornstein-Zernike equation in the Percus-Yevick approximation, and showed that the system undergoes a liquid-gas phase transition (see Fig. 11). On the other hand, Chiew and Glandt (1983) used the approach proposed by Coniglio and his collaborators (1977a) (see section 5.1.2) to locate the percolation line in the phase diagram of the sticky-hard-sphere model. As is shown in Fig. 11, this line does not pass by the critical point. However, following Kranendonk and Frenkel (1988), we note that its location for extreme values of the volume fraction³⁰ casts some doubt upon the adequacy of the Percus-Yevick approximation. Indeed, the percolation line starts at $\phi = 0$, predicting the existence of a percolating cluster in vacuum, and goes to the unphysical value $\phi = 1$, greater than the close packing volume fraction. In contrast, Monte-Carlo simulation predictions show that the percolation line *starts* very close to the critical point and goes through the supercritical phase as in the case of a Lennard-Jones fluid (Seaton and Glandt, 1987a; Kranendonk and Frenkel, 1988). According to Kranendonk and Frenkel (1988), the prolongation of the percolation line under the coexistence curve should be taken with caution.

6 Summary and outlook

Ever since Mayer proposed his theory of condensation in 1937, the correspondence between thermodynamics and the morphology of simple fluids in terms of clusters has attracted a lot of interest. In this last section, we summarize the various stages of this research area, and close by mentioning some open questions.

³⁰ The volume fraction is related to the density by $\phi = \pi\rho\sigma^3/6$, where σ is the diameter of the particles.

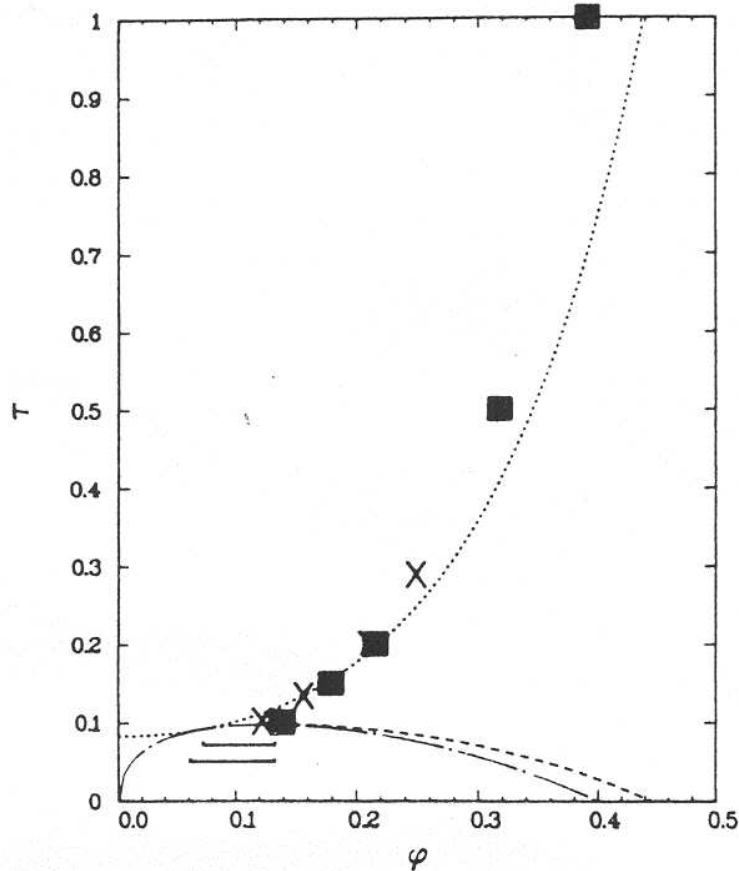


Fig. 11. Phase diagram of the sticky-hard-sphere model. The stickiness parameter τ (vertical axis) is a measure of the temperature and ϕ is the volume fraction (horizontal axis). The dashed line represents the spinodal line in the Percus-Yevick approximation. The percolation line determined by the Percus-Yevick approximation, dotted line (Chiew and Glandt, 1983), and by numerical simulations, black squares (Kranendonk and Frenkel, 1988), and crosses (Seaton and Glandt, 1987a,b). The horizontal bars give the positions of percolation thresholds below the spinodal line (from Kranendonk and Frenkel, 1988).

Initially, the purpose was to introduce clusters as tools in order to calculate the thermodynamic quantities of a classical fluid, and in particular to study the liquid-gas phase transition and the critical point. To this end, condensation is defined as the formation of a macroscopic cluster. By considering a real fluid as a gas of non-interacting clusters, one can write the equation of state of the system as a function of the cluster size distribution. Consequently, the mean cluster size varies like the compressibility and then should diverge at, and only at, the thermodynamic critical point. This is the case by construction for Fisher droplets which provide a morphological description of the critical point. But these phenomenological non-interacting clusters cannot be identified as sets of particles in the fluid. The next step was to find a microscopic definition of clusters that behave like Fisher droplets.

In the lattice-gas model, the problem amounts to finding a definition of clusters that produces a percolation threshold at the critical point. Ising clusters, defined by the simple criterion of proximity in real space, do not fulfill this condition. In contrast, Coniglio-Klein clusters, whose definition is based on the mathematical work of Fortuin and Kasteleyn, are explicitly designed to this end. But this is not the end of the story: Coniglio-Klein clusters exhibit a percolation behaviour not only at the critical point, but also along the so-called “Kertész line” which goes through the supercritical region of the phase diagram. Within the context of the perfect gas of clusters model, this percolation line should imply forbidden thermodynamic singularities. However, because Coniglio-Klein clusters do not form a perfect gas of clusters, there is no valid reason for eliminating the Kertész line. It remains to give a physical interpretation of this percolation line. This is what Campi and Krivine have done by showing that Coniglio-Klein clusters are self-bound on average. This interpretation in terms of self-bound clusters opens up a new field of investigation.

Self-bound clusters can be studied in the more realistic framework of a Lennard-Jones fluid. It is interesting to notice that these clusters were introduced not to provide a correspondence between thermodynamics and geometry, but rather to describe processes like the fragmentation of a piece of matter. Nevertheless, self-bound clusters strikingly present the morphological manifestations associated with the liquid-gas phase transition, and therefore can be considered as the microscopic physical counterparts of the phenomenological Fisher droplets. What is more, self-bound clusters give rise to a percolation line in the supercritical phase. An important open question, which arises from their definition based on physical grounds, is whether this line could be observed in real fluids.

Various real systems behaving like simple fluids can be used to search for signals of the self-bound clusters and the percolation line. For example, the effusion of a fluid through a pin hole allows one to infer the cluster size distribution from the mass yield of escaped clusters with a given velocity. Hence, the presence of clusters (dimers and trimers) was found in the gas phase at very low density (Miller and Kusch, 1955, 1956). However, this kind of experiment seems to be inappropriate to explore a fluid at high density, in the region of the percolation line. On the other hand, experiments dealing with binary fluids (which belong to the universality class of the $3d$ Ising model (Chen *et al.*, 1983)) were performed to give a morphological description of the critical point in terms of clusters (Guenoun *et al.*, 1989). The relationship between these clusters, defined from persistent density fluctuations and the self-bound clusters is not yet understood. Very recently, a sharp decrease of H^+ ion mobility in a mixture of isobutyric acid and water has been ascribed to a percolation line of “dynamic clusters” which starts at the critical point (Bonn *et al.*, 2002). At first glance, the vertical position of this curve in the

phase diagram would suggest a closer connection with configurational clusters (see Fig. 5 in (Bonn *et al.*, 2002)). However, the slope of the percolation line of the self-bound clusters may depend on the system considered. The question of whether these “dynamic clusters” are self-bound, still awaits an answer.

From a rather different perspective, the relation between clustering and thermodynamics is critical to the determination of the phase diagram of small systems, like atomic nuclei and aggregates (Hill, 1963). In a first approximation, the nuclear interaction can be seen as a two body potential with a repulsive hard-core and a short-ranged attraction. By disregarding quantum effects at high enough energy, hot nuclear matter is thought to behave like a classical simple fluid (Bondorf *et al.*, 1995; Das Gupta *et al.*, 2001, and references therein). A crucial question which then arises is whether traces of a liquid-gas phase transition can be observed in an atomic nucleus (Siemens, 1983) ? A direct observation of such a signal is of course quite arduous in a small system, and today there is still no conclusive answer to this question.

To explore the phase diagram of nuclear matter, atomic nuclei are heated and compressed by collisions at high bombarding energy (about 100 MeV/nucleon) with other nuclei. As a result, an excited nucleus expands and breaks into fragments which can be detected using 4π multidetectors (see references in Bondorf *et al.*, 1995). Basically, only the fragment size and the kinetic energy distributions can be directly measured. The challenge is then to infer the thermodynamical state of the system before fragmentation occurs from these two distributions which characterize the asymptotic fragments.

To this end, several theoretical approaches have been proposed. “Statistical Equilibrium Models”, like the SMM (Bondorf *et al.*, 1995) and the MMMC (Gross, 1997) models, assume that at a given stage of the expansion the system is an ensemble of non-interacting spherical fragments. Using the perfect gas of clusters model, and some elements of nuclear physics, these models have been successful in describing the observed fragment size distributions (Botvina *et al.*, 1995). However, the kinetic energies are too low compared to experimental data, and worst of all, the strongly restrictive hypotheses of the perfect gas of clusters prevent exploration of the high density region of the phase diagram. On the other hand, classical molecular dynamics simulations of the expansion and fragmentation of a small system allow one to investigate the whole phase diagram (Schlagel and Pandharipande, 1987; Belkacem *et al.*, 1995; Chernomoretz *et al.*, 2001; Campi *et al.*, 2002b). In this way, it has been shown that self-bound clusters in the hot and dense fluid are the precursors of the observed fragments (Dorso and Randrup, 1993; Campi *et al.*, 2001b, 2002b). In particular, self-bound clusters in the initial system and asymptotic fragments have the same size distribution. The initial thermodynamic state could be deduced from the measured quantities by using the correspondence between the phase diagram and the self-bound cluster size distribution at

equilibrium (Campi *et al.*, 2002b). It must be emphasized that various experiments of fragmentation of atomic nuclei³¹ and atomic aggregates (Farizon *et al.*, 1998; Gobet *et al.*, 2001) exhibit a percolation behaviour of the fragment size distribution (U-shapes, power law, and exponentials at respectively low, intermediate, and high energy).

Finally, beyond the framework of simple fluids, attractive colloidal suspensions display aggregation and dynamic behaviours that could be understood in terms of self-bound clusters. Compared with atoms, colloidal particles have larger sizes, a slower diffusion, and a range of attraction much smaller than the hard-core diameter (Pusey, 1991; Anderson and Lekkerkerker, 2002). These features contribute to form morphological structures that can be visualized by using microscopic imaging (Segrè *et al.*, 2001). We are not aware of a microscopic theoretical description of these clusters. What is more, percolation lines are frequently observed in attractive colloidal suspensions. According to the particular physical situation, the percolation threshold is associated with a sharp change in the following quantities (Coniglio, 2001): i) Electrical conductivity in water-in-oil microemulsions (Chen *et al.*, 1994; Weigert *et al.*, 1997), ii) Viscosity of triblock copolymer micellar solutions (Mallamace *et al.*, 1999, 2001), iii) Elastic modulus of dispersions of silica spheres grafted with polymer chains (Grant and Russel, 1993), and iv) Correlation functions, measured by dynamic light scattering, of dispersions of silica spheres coated with stearyl alcohol (Verduin and Dhont, 1995). It is worth noting that in all these cases the percolation line passes in the vicinity of the critical point. Therefore, clustering seems to be intimately related to the dynamic properties of complex fluids. Clearly, more work is needed in this direction.

Acknowledgments

I am deeply grateful to my collaborators Xavier Campi and Hubert Krivine. During the writing of this article, I have benefited from fruitful discussions with Antonio Coniglio to whom I am thankful. I wish also to thank Donald Sprung for making useful remarks about the manuscript. This work was supported by grants from NSERC Canada (research grant SAPIN-3198) and from the European TMR Network-Fractals (Postdoctoral Grant, Contract No. FMRXCT-980183).

³¹ See for example (Finn *et al.*, 1982; Campi, 1988; Gilkes *et al.*, 1994; Schüttauf *et al.*, 1996; Campi *et al.*, 2000; Kleine Berkenbusch *et al.*, 2002).

A Perfect gas of clusters model

Let us consider a set of non-interacting clusters that do not have any volume. The n_s indistinguishable clusters of size s form a chemical species characterized by their mass ms , their chemical potential μ_s and the partition function $q_s(T, V)$.

In the canonical ensemble, at constant volume and temperature, the differential of the free energy is

$$dF = \sum_s \mu_s dn_s.$$

Furthermore, mass conservation is ensured by the condition $\sum sn_s = N$, or $\sum sdn_s = 0$. Chemical equilibrium between clusters implies the minimization of the free energy. By the method of Lagrangian multipliers, we obtain

$$\mu_s = s\mu \quad \text{for} \quad s = 1, 2, \dots, N \quad (\text{A.1})$$

where μ is the particle chemical potential. The fugacity z_s of clusters of size s is then

$$z_s = e^{\beta\mu_s} = e^{\beta s\mu} = z^s$$

where $z = z_1$ is the fugacity of the particles. The partition function for a given partition $\vec{P} = \{n_1, n_2, \dots\}$ of particles into non-interacting clusters is given by

$$Q_{\vec{P}}(T, V) = \prod_{s=1}^{\infty} \frac{q_s^{n_s}}{n_s!}. \quad (\text{A.2})$$

The total partition function of a system of N particles is then

$$Q_N(T, V) = \sum_{\vec{P}} Q_{\vec{P}} \delta(\sum sn_s - N)$$

where $\sum_{\vec{P}}$ is a sum over all the possible partitions, whatever the number of particles. By moving over to the grand canonical ensemble, the grand partition function $\Xi(z, T, V)$ can be written as a function of the fugacity z :

$$\begin{aligned} \Xi(z, T, V) &= \sum_{N \geq 0} z^N Q_N \\ &= \sum_{N \geq 0} z^N \sum_{\vec{P}} Q_{\vec{P}} \delta(\sum sn_s - N) \\ &= \sum_{N \geq 0} \sum_{\vec{P}} z^N \prod_{s=1}^{\infty} \frac{q_s^{n_s}}{n_s!} \delta(\sum sn_s - N). \end{aligned}$$

By summing over N , we obtain

$$\begin{aligned}
\Xi(z, T, V) &= \sum_{\vec{p}} \prod_{s=1}^{\infty} z^{sn_s} \prod_{s=1}^{\infty} \frac{q_s^{n_s}}{n_s!} \\
&= \sum_{\vec{p}} \prod_{s=1}^{\infty} \frac{(q_s z^s)^{n_s}}{n_s!} \\
&= \prod_{s=1}^{\infty} \sum_{n_s=0}^{\infty} \frac{(q_s z^s)^{n_s}}{n_s!} \\
&= \prod_{s=1}^{\infty} e^{q_s z^s} \\
&= e^{\sum_{s=1}^{\infty} q_s z^s}.
\end{aligned} \tag{A.3}$$

The grand partition function $\Xi(z, T, V)$ allows us to calculate the grand potential $\Omega = F - \mu N = -kT \ln \Xi(z, T, V)$. Because $\Omega = -PV$ (see for example Landau and Lifshitz, 1959), we infer the pressure and the density in the thermodynamic limit:

$$\beta P \equiv \lim_{V \rightarrow \infty} \left(\frac{1}{V} \ln \Xi \right) = \lim_{V \rightarrow \infty} \left(\frac{1}{V} \sum_{s=1}^{\infty} q_s(T, V) z^s \right) \tag{A.4}$$

$$\rho \equiv \lim_{V \rightarrow \infty} \left(\frac{z}{V} \frac{\partial \ln \Xi}{\partial z} \right) = \lim_{V \rightarrow \infty} \left(\frac{1}{V} \sum_{s=1}^{\infty} s q_s(T, V) z^s \right). \tag{A.5}$$

For large enough volume, $q_s(T, V)/V$ becomes independent of V and tends to $\tilde{q}_s(T)$. In the domain of convergence of series (A.4) and (A.5), we can permute the limit when $V \rightarrow \infty$ and the sum over s . The pressure and density expression are then given by

$$\begin{aligned}
\beta P &= \sum_{s=1}^{\infty} \tilde{q}_s(T) z^s \\
\rho &= \sum_{s=1}^{\infty} s \tilde{q}_s(T) z^s.
\end{aligned}$$

It is convenient to express the thermodynamic quantities as functions of the series $\pi(T, z)$ (Fisher, 1967a):

$$\begin{aligned}
\pi(T, z) &\equiv \sum_{s=1}^{\infty} \tilde{q}_s(T) z^s \\
\pi^{(n)}(T, z) &\equiv \left(z \frac{\partial}{\partial z} \right)^{(n)} \pi(T, z).
\end{aligned}$$

The expressions for pressure, density, compressibility, and specific heat at constant volume, become

$$\begin{aligned}
\beta P &= \pi(T, z) \\
\rho &= \pi^{(1)}(T, z) \\
\chi T &\equiv \frac{1}{\rho} \frac{\partial \rho}{\partial P} = \frac{1}{\rho} \frac{\partial \rho}{\partial z} \frac{\partial z}{\partial P} = \frac{\beta}{\rho^2} \pi^{(2)}(T, z) \\
C_v &= T \frac{\partial S}{\partial T_V} = -T \frac{\partial^2 \Omega}{\partial T^2_{V,\mu}} = kT^2 V \frac{\partial^2 \pi(T, z)}{\partial T^2_{V,\mu}}.
\end{aligned}$$

Let us calculate the cluster size distribution. From now on, n_s is the *mean* number of clusters of size s :

$$n_s = z_s \frac{\partial \ln \Xi}{\partial z_s}.$$

From Eq. (A.1) and Eq. (A.3) we obtain

$$n_s = z_s q_s = q_s z^s.$$

Define m_k as the moment of order k of the cluster size distribution:

$$m_k = \sum_{s=1}^{\infty} s^k n_s.$$

In this theoretical framework, thermodynamic quantities are associated with the moments m_k . Indeed,

$$\begin{aligned}
\pi(T, z)^{(n)} &= \frac{1}{V} \sum_{s=1}^{\infty} s^n q_s z^s \\
&= \frac{1}{V} \sum_{s=1}^{\infty} s^n n_s = \frac{m_n(T, z)}{V}.
\end{aligned}$$

We then have

$$\beta P = \frac{m_0(T, z)}{V} \tag{A.6}$$

$$\rho = \frac{m_1(T, z)}{V} = \frac{N}{V} \tag{A.7}$$

$$\chi = \frac{\beta m_2(T, z)}{V \rho^2} = \frac{V}{kT} \frac{m_2(T, z)}{m_1^2(T, z)} \tag{A.8}$$

$$C_v = kT^2 \frac{\partial^2 m_0}{\partial T^2_{V,\mu}}. \tag{A.9}$$

From Eqs. (A.6) and (A.8) it follows that³²:

$$P\chi = \frac{m_0 m_2}{m_1^2} = \gamma_2$$

where γ_2 is a quantity that diverges as m_2 at the percolation threshold (Campi, 1988).

Equations (A.6)-(A.9) clearly show that in a perfect gas of clusters model, geometric and thermodynamic quantities must diverge at the same points of the phase diagram. In particular, the second moment of the cluster size distribution diverges like the compressibility.

B Stability of the probabilistic Hill clusters

To begin, we define the stability against particle emission. The separation energy $e_i^{C_s}$ is the energy of a particle i calculated in the center of mass system of the cluster C_s to which it belongs. A cluster is stable against particle emission if, for each particle i belonging to C_s , we have:

$$e_i^{C_s} \equiv K_i^* + \sum_{j \in C_s, j \neq i} u(r_{ij}) < 0$$

where K_i^* is the kinetic energy of particle i calculated in the center of mass system of cluster C_s , that is

$$K_i^* = \frac{m}{2}(\vec{v}_i - \vec{V}^{C_s})^2,$$

and $\vec{V}^{C_s} = (\sum_{i \in C_s} \vec{v}_i)/s$ is the velocity of the center of mass of the cluster C_s . When the positions and velocities of the particles belonging to a given cluster are known, this criterion is straightforward to check.

Let us now show that probabilistic Hill clusters are stable on average against particle emission in the lattice-gas model (Campi and Krivine, 1997). To this end, we evaluate the average sign of the separation energy. For large enough clusters, the velocity of the center of mass can be neglected. The relative kinetic energy of a particle is then equal to $mv_i^2/2$, where v_i is randomly given by the Maxwell distribution of variance $1/\beta m$. First consider the case of a particle interacting with only one other particle of the cluster. Its separation energy is then given by

$$e_i = \frac{m}{2}v_i^2 - \epsilon.$$

³² In a perfect gas of *particles*, there are only monomers: $m_0 = m_1 = m_2 = N$ and $\chi = 1/P$.

Because the particle belongs to the cluster, we have by definition of a Hill's bond $e_i < 0$. Now, suppose the particle interacts with two particles of the cluster (see Fig. B.1). The separation energy of the particle is

$$e_i = \frac{m}{2}v_i^2 - 2\epsilon.$$

The probability that e_i is negative is $Pr(mv_i^2/2 \leq 2\epsilon) = p_{Hill}(2\beta\epsilon)$. On the other hand, the probability that the particle is linked to the cluster either by one or two independent bonds is given by

$$2p_{Hill}(\beta\epsilon) - p_{Hill}^2(\beta\epsilon).$$

According to Eq. (24), we can substitute p_{ck} for p_{Hill} . It is then very simple to check that

$$2p_{ck}(\beta\epsilon) - p_{ck}^2(\beta\epsilon) = p_{ck}(2\beta\epsilon).$$



Fig. B.1. Particle i interacts with two particles of the cluster it belongs to. 1) Particle i is linked to the cluster by only one Hill's bond (heavy line) with particle k , but interact also with particle j . 2) Particle i is linked to the cluster by two Hill's bonds to particles k and j .

The generalization to more bonds between the particle and the cluster is straightforward. In conclusion, if a particle belongs to a probabilistic Hill cluster, its separation energy is negative. The condition for stability against particle emission is fulfilled on average.

References

- Abraham, F.F., 1974, J. Chem. Phys. **61**, 1221.
 Abraham, F.F., and J.A. Barker, 1975, J. Chem. Phys. **63**, 2266.
 Adler, J., and D. Stauffer, 1991, Physica A **175**, 222.
 Alexandrowicz, Z., 1988, Phys. Rev. Lett. **60**, 669.
 Alexandrowicz, Z., 1989, Physica A **160**, 310.
 Allen, M.P., and D.J. Tildesley, 1987, Computer Simulation of Liquids (Oxford University Press, Oxford).
 Anderson, V.J., and H.N.W. Lekkerkerker, 2002, Nature **416**, 811.

- Band, W., 1939a, J. Chem. Phys. **7**, 324.
- Band, W., 1939b, J. Chem. Phys. **7**, 927.
- Baxter, R.J., 1968, J. Chem. Phys. **49**, 2770.
- Belkacem, M., V. Latora, and A. Bonasera, 1995, Phys. Rev. C **52**, 271.
- Bijl, A., 1938, Ph.D. thesis, Leiden, Discontinuities in the Energy and Specific Heat.
- Binder, K., 1975, J. Chem. Phys. **63**, 2265.
- Binder, K., 1976a, Ann. Phys. (N.Y.) **98**, 390.
- Binder, K., 1976b, in Phase Transitions and Critical Phenomena, Volume 5b, edited by C. Domb and M.S. Green (Academic Press, London, New York, San Francisco), p. 72.
- Bondorf, J.P., A.S. Botvina, A.S. Iljinov, I.N. Mishustin, and K. Sneppen, 1995, Phys. Rep. **257**, 133.
- Bonn, D., D. Ross, S. Hachem, S. Gridel and J. Meunier, 2002, Europhys. Lett. **58**, 74.
- Botvina, A.S., *et al.*, 1995, Nucl. Phys. A **584**, 737.
- Bug, A.L.R., S.A. Safran, G.S. Grest, and I. Webman, 1985, Phys. Rev. Lett. **55**, 1896.
- Caccamo, C., 1996, Phys. Rep. **274**, 1.
- Cagniard de La Tour, 1822, Annales de Chimie **21**, 127 and 178.
- Campi, X., 1988, Phys. Lett. B **208**, 351.
- Campi, X., and H. Krivine, 1997, Nucl. Phys. A **620**, 46.
- Campi, X., H. Krivine, and J. Krivine, 2002a, "Clustering and Thermodynamics in the Lattice-Gas Model", to be published in Physica A.
- Campi, X., H. Krivine, E. Plagnol, and N. Sator, 2000, Eur. J. Phys. D **11**, 233.
- Campi, X., H. Krivine, E. Plagnol, and N. Sator, 2002b, in Proceedings of the XL International Winter Meeting on Nuclear Physics, Bormio Italy, edited by I. Iori and A. Moroni (Università degli studi di Milano, Italy), p. 161.
- Campi, X., H. Krivine, and A. Puente, 1999, Physica A **262**, 328.
- Campi, X., H. Krivine, and N. Sator, 2001a, Physica A. **296**, 24.
- Campi, X., H. Krivine, and N. Sator, 2001b, Nucl. Phys. A **681**, 458c.
- Chandler, D., 1987, Introduction to Modern Statistical Mechanics, (Oxford University Press, Oxford).
- Chen, S.H., C.C. Lai, J. Rouch, and P. Tartaglia, 1983, Phys. Rev. A **27**, 1086.
- Chen, S.H., J. Rouch, F. Sciortino, and P. Tartaglia, 1994, J. Phys.: Condens. Matter **6**, 10855.
- Chernomoretz, A., M. Ison, S. Ortiz, and C.O Dorso, 2001, Phys. Rev. C **64**, 024606.
- Chiew, Y.C., and E.D. Glandt, 1983, J. Phys. A **16**, 2599.
- Coniglio, A., 1975, J. Phys. A **8**, 1773.
- Coniglio, A., 1976, Phys. Rev. B **13**, 2194.
- Coniglio, A., 2001, J. Phys.: Condens. Matter **13**, 9039.
- Coniglio, A., U. De Angelis, A. Forlani, 1977a, J. Phys. A **10**, 1123.
- Coniglio, A., U. De Angelis, A. Forlani, and G. Lauro, 1977b, J. Phys. A **10**,

- 219.
- Coniglio, A., F. de Liberto, G. Monroy, and F. Peruggi, 1989, J. Phys. A **22**, L837.
- Coniglio, A., and W. Klein, 1980, J. Phys. A **13**, 2775.
- Coniglio, A., C.R. Nappi, F. Peruggi and L. Russo, 1977c, J. Phys. A **10**, 205.
- Das Gupta, S., A.Z. Mekjian, M.B. Tsang, 2001, "Liquid-gas phase transition in nuclear multifragmentation", in Advances in Nuclear Physics, Volume **26**, edited by J.W. Negele and E. Vogt Uitgever (Plenum Press, New York) and nucl-th/0009033.
- Dorso, C., and J. Randrup, 1993, Phys. Lett. B **301**, 328.
- Drory, A., 1996, Phys. Rev. E **54**, 5992.
- Essam, J.W., and M.E. Fisher, 1963, J. Chem. Phys. **38**, 802.
- Farizon, B., *et al.*, 1998, Phys. Rev. Lett. **81**, 4108.
- Finn, J.E., *et al.*, 1982, Phys. Rev. Lett. **49**, 1321.
- Fisher, M.E., 1967a, Physics **3**, 255.
- Fisher, M.E., 1967b, J. Appl. Phys. **38**, 981.
- Fisher, M.E., 1971, in Critical Phenomena, Proceedings of the International School of Physics "Enrico Fermi" Course LI, Varenna on Lake Como Italy, edited by M. S. Green (Academic, New York), p. 1.
- Fisher, M.E., and B. Widom, 1969, J. Chem. Phys. **50**, 3756.
- Fortuin, C.M., and P.W. Kasteleyn, 1972, Physica **57**, 536.
- Fortunato, S., 2002, Phys. Rev. B **66**, 054107.
- Frenkel, J., 1939a, J. Chem. Phys. **7**, 200.
- Frenkel, J., 1939b, J. Chem. Phys. **7**, 538.
- Geiger, A., and H.E. Stanley, 1982, Phys. Rev. Lett. **49**, 1895.
- Gilkes, M.L., *et al.*, 1994, Phys. Rev.Lett. **73**, 1590.
- Gobet, F., *et al.*, 2001, Phys. Rev.Lett. **87**, 203401.
- Goldenfeld, N., 1992, Lectures on Phase Transitions and Renormalization Group (Addison-Wesley).
- Grant, M.C., and W.B. Russel, 1993, Phys. Rev. E **47**, 2606.
- Gross, D.H.E., 1997, Phys. Rep. **279**, 119.
- Guenoun, P., F. Perrot and D. Beysens, 1989, Phys. Rev. Lett. **63**, 1152.
- Hansen, J.P., and I.R. McDonald, 1986, Theory of Simple Liquids (Academic, London/New York).
- Harrison, S.F., and J.E. Mayer, 1938, J. Chem. Phys. **6**, 101.
- Heermann, D.W., A. Coniglio, W. Klein, and D. Stauffer, 1984, J. Stat. Phys. **36**, 447.
- Heermann, D.W., and D. Stauffer, 1981, Z. Phys. B **44**, 339.
- Heyes, D.M., and J.R. Melrose, 1988, J. Phys. A **21**, 4075.
- Heyes, D.M., and J.R. Melrose, 1989, Mol. Phys. **66**, 1057.
- Hill, T.L., 1955, J. Chem. Phys. **23**, 617.
- Hill, T.L., 1963, Thermodynamics of Small Systems (Benjamin, New York), Chap 5.
- Hu, C.K., 1984, Phys. Rev. B **29**, 5103.
- Huang, K., 1987, Statistical Mechanics (John Wiley and Sons, New York).

Jan, N., A. Coniglio and D. Stauffer, 1982, J. Phys. A **15**, L699.
 Kasteleyn, P.W., and C.M. Fortuin, 1969, J. Phys. Soc. Jpn. **26**, 11.
 Kertész, J., 1989, Physica A **161**, 58.
 Kiang, C.S., 1970, Phys. Rev. Lett. **24**, 47.
 Kiang, C.S., and D. Stauffer, 1970 Z. Phys. **235**, 130.
 Kirkpatrick, S., 1984, J. Stat. Phys. **34**, 975.
 Klein, W., 1990, Phys. Rev. Lett. **65**, 1462.
 Klein, W., H.E. Stanley, P.J. Reynolds and A. Coniglio, 1978, Phys. Rev. Lett. **41**, 1145.
 Kleine Berkenbusch, M., *et al.*, 2002, Phys. Rev. Lett. **88**, 022701.
 Kranendonk, W.G.T., and D. Frenkel, 1988, Mol. Phys. **64**, 403.
 Landau, L.D., and E.M. Lifshitz, 1959, Statistical Physics (Pergamon, Oxford/New York).
 Lee, J.K., J.A. Barker and F.F. Abraham, 1973, J. Chem. Phys. **58**, 3166.
 Lee, T.D. and C.N. Yang, 1952, Phys. Rev. **87**, 410.
 Liverpool, T.B., and S.C. Glotzer, 1996, Phys. Rev. E **53**, R4255.
 Luzar, A., and D. Chandler, 1996, Phys. Rev. Lett. **76**, 928.
 Mallamace, F., R. Beneduci, P. Gambadauro, D. Lombardo, and S.H. Chen, 2001, Physica A **302**, 202.
 Mallamace, F., S.H. Chen, Y. Liu, L. Lobry, and N. Micali, 1999, Physica A **266**, 123.
 Mayer, J.E., 1937, J. Chem. Phys. **5**, 67.
 Mayer, J.E., and P.G. Ackermann, 1937, J. Chem. Phys. **5**, 74.
 Mayer, J.E., and S.F. Harrison, 1938, J. Chem. Phys. **6**, 87.
 Mayer, J.E., and M.G. Mayer, 1940, Statistical Mechanics (John Wiley and Sons, New York/Toronto).
 Miller, R.C., and P. Kusch, 1955, Phys. Rev. **99**, 1314.
 Miller, R.C., and P. Kusch, 1956, J. Chem. Phys. **25**, 860.
 Müller-Krumbhaar, H., 1974a, Phys. Lett. A **48**, 459.
 Müller-Krumbhaar, H., 1974b, Phys. Lett. A **50**, 27.
 Müller-Krumbhaar, H., and E. Stoll, 1976, J. Chem. Phys. **65**, 4294.
 Nishikawa, K., and T. Morita, 2000, Chem. Phys. Lett. **316**, 238.
 Odagaki, T., N. Ogita and H. Matsuda, 1975, J. Phys. Soc. Jpn. **39**, 618.
 Ottavi, H., 1981, Z. Phys. B **44**, 203.
 Pan, J., and S. Das Gupta, 1995, Phys. Rev. C **51**, 1384.
 Pathria, R.K., 1972, Statistical Mechanics (Pergamon, Oxford/Toronto).
 Puente, A., 1999, Phys. Lett. A **260**, 234.
 Pugnali, L.A., and F. Vericat, 2000, Phys. Rev. E **61**, R6067.
 Pugnali, L.A., I.F. Márquez, and F. Vericat, 2002, "Continuum percolation of simple fluids: Energetic connectivity criteria", preprint, cond-mat/0209534.
 Pusey, P.N., 1991, in Liquids, Freezing and Glass Transition, Les Houches Session LI 1989, edited by J.P. Hansen, D. Levesque, and J. Zinn-Justin (North-Holland, Amsterdam), p. 763.
 Rathjen, W., D. Stauffer, and C.S. Kiang, 1972, Phys. Lett. A **40**, 345.

Ray, T.S., and J.S. Wang, 1990, *Physica A* **167**, 580.

Reatto L., 1970, *Phys. Lett. A* **33**, 519.

Reiss, H., J.L. Katz, and E.R. Cohen, 1968, *J. Chem. Phys.* **48**, 5553.

Reiss, H., A. Tabazadeh, and J. Talbot, 1990, *J. Chem. Phys.* **92**, 1266.

Roussenq, J., A. Coniglio and D. Stauffer, 1982, *J. Phys. (Paris)* **43**, L703.

Ruelle, D., 1969, *Statistical Mechanics, Rigorous Results* (Benjamin, New York).

Safran, S.A., I. Webman, and G.S. Grest, 1985, *Phys. Rev. A* **32**, 506.

Sator, N., 2000, Ph.D. thesis number 6224 (University of Orsay).

Schioppa, C.P., F. Sciortino and P. Tartaglia, 1998, *Phys. Rev. E* **57**, 3797.

Schlagel, T.J., and V.R. Pandharipande, 1987, *Phys. Rev. C* **36**, 162.

Schütteauf, A., *et al.*, 1996, *Nucl. Phys. A* **607**, 457.

Seaton, N.A., and E.D. Glandt, 1987a, *J. Chem. Phys.* **86**, 4668.

Seaton, N.A., and E.D. Glandt, 1987b, *PhysicoChem. Hydrodyn.* **9**, 396.

Segrè, P.N., V. Prasad, A.B. Schofield, and D.A. Weitz, 2001, *Phys. Rev. Lett.* **86**, 6042.

Siemens, P.J., 1983, *Nature* **305**, 410.

Soto, R., and P. Cordero, 1997, *Phys. Rev. E* **56**, 2851.

Soto, R., and P. Cordero, 1998a, *Physica A* **257**, 521.

Soto, R., and P. Cordero, 1998b, *J. Chem. Phys.* **108**, 8989.

Starr, F.W., J.K. Nielsen, and H.E. Stanley, 1999 *Phys. Rev. Lett.* **82**, 2294.

Stauffer, D., 1981, *J. Phys. (Paris)* **42**, L99.

Stauffer, D., 1990, *Physica A* **168**, 614.

Stauffer, D., and A. Aharony, 1994, *Introduction to percolation theory* (Taylor and Francis, London/Bristol).

Stauffer, D., and C.S. Kiang, 1971, *Phys. Rev. Lett.* **27**, 1783.

Stauffer, D., C.S. Kiang, and G.H. Walker, 1971, *J. Stat. Phys.* **3**, 323.

Stillinger Jr, F.H., 1963, *J. Chem. Phys.* **38**, 1486.

Stoll, E., K. Binder, and T. Schneider, 1972, *Phys. Rev. B* **6**, 2777.

Swendsen, R.H., and J.S. Wang, 1987, *Phys. Rev. Lett.* **58**, 86.

Sykes, M.F., and D.S. Gaunt, 1976, *J. Phys. A* **9**, 2131.

Verduin, H., and J.K.G. Dhont, 1995, *J. Colloid Interface Sci.* **172**, 425.

Wang, J.S., 1989, *Physica A* **161**, 249.

Wang, J.S., and R.H. Swendsen, 1990, *Physica A* **167**, 565.

Weigert, S., H.F. Eicke, and W. Meier, 1997, *Physica A* **242**, 95.

Wu, F.Y., 1982, *Rev. Mod. Phys.* **54**, 235.

Xu, J., and G. Stell, 1988, *J. Chem. Phys.* **89**, 1101.

Yang, C.N., and T.D. Lee, 1952, *Phys. Rev.* **87**, 404.

Yang, Y.S., and C.J. Thompson, 1998, *Physica A* **248**, 185.